



THE UNIVERSITY  
*of* EDINBURGH

MSc Sustainable Energy Systems

**Wake deficit simulation and  
techno-economic feasibility assessment of  
dynamically positioned floating offshore wind  
turbines**

by  
Seamus Flannery

2024

**MSc Dissertation Thesis**  
**MSc in Sustainable Energy Systems**

---

**Wake deficit simulation and techno-economic feasibility assessment of dynamically positioned floating offshore wind turbines**

Seamus Flannery  
S2523602  
August, 2024



# Investigating Dynamic Positioning in Floating Offshore Wind Farms

## Mission Statement

Student: Seamus Flannery

Matric. No.: s2523602

Supervisor: Andrew Lyden

### Summary and initial literature review

Floating offshore wind turbines are likely to be the next large-scale renewable source of energy. Offshore wind turbines are beneficial as they avoid taking up land space, dealing with onshore regulation, residences, and infrastructure, and have access to higher and less turbulent winds. However, there is relatively little space for fixed-bed offshore wind turbines, which make up the majority of current commercial offshore wind generation, as these turbines require shallow waters (less than 50m); the potential resource for floating offshore wind farms is enormous [1]. However, there are many challenges associated with floating offshore wind turbines. Floating wind is expensive, and it is technically and financially challenging to moor turbines to the seafloor. The ocean is a harsh environment and floating turbines, and their anchoring systems undergo huge wind and wave forces [2]. The costs of mooring systems might be reducible by mooring turbines in shared mooring configurations, reducing the number of anchors required [3]. Shared mooring must however cope with the ability for floating platforms to move around the ocean surface, simultaneously keeping turbines anchored to the seafloor, and keeping them from colliding. Mooring and cabling were cited as target areas for innovation by joint industry research groups [4]. Another challenge with all wind turbines is turbine wake loss, wherein turbines disturb the flow of air incident on turbines downwind from them, reducing the yields by up to 40% for the downwind turbines [5]. Because wakes are incident on turbines directly downwind from them, predominant wind conditions and the orientation of turbines within a farm are huge factors in the ultimate yield of a farm, so layouts need to be optimised [6]. This means however, that a farm with statically positioned turbines is vulnerable to significant loss in wind directions that aim wakes into downwind turbines.

### Main aims and objectives

The aim of this dissertation is to investigate if there is any value to allowing or directing floating offshore wind turbines to move, on an hourly timescale, within a farm, in order to minimize wake losses. This dissertation may take the form of a global opportunity study. The primary objective is to measure the potential benefit of reduced wake losses due to mobility/variable farm orientations and weigh those benefits against the technical and economic constraints of implementing such a farm. This will allow us to determine if this topic is worthy of further investigation, and what the global opportunity for offshore wind firms is.

### Interim targets

My first interim target, which will be ongoing throughout the semester will be to conduct literature review in support of the modelling I'm performing. In parallel, I will begin working on assessing sensitivity on wake loss percentage to factors like wind characterization, ocean depth, etc. I will also need to create methods for testing a variety of farm designs and orientations that can represent turbines which shift on an hourly scale. Using those methods, I will characterize the wake loss benefits (if they exist) of having repositionable farm spacings, using PyWake and ERA5 weather information. I will also need to assess what would the potential mooring costs look like to support a farm which had mobile turbines like this. This assessment should at a minimum determine the bounds on what the cost of such a mooring system would be, as well as the engineering feasibility of such a system, but could also describe or investigate potential specific mooring designs. I will use the results of this work to assess the overall economic feasibility of such a farm



# **Declaration**

This project report is submitted in partial fulfilment of the requirements for the degree of MSc Sustainable Energy Systems. I declare that this thesis is my original work, except where stated otherwise. This thesis has never been submitted for any degree or examination to any other University.

*Seamus Flannery*

This thesis was conducted under the supervision of Dr Andrew Lyden.

# Abstract

This thesis examines the viability of dynamically repositioning floating wind turbines as a turbine wake management strategy. Dynamically repositioning floating offshore wind farms were simulated in PyWake to compare energy yield against the yield of static farms. This test was performed with time-series wind data from a variety of sites around the world with different wind direction and wind speed distributions. The tests establish that the technique is capable of managing turbine wake effects to conservatively improve turbine yield by up to 2.4% for a 5-by-5 turbine array of NREL 15MW standard turbines, relative to a fixed-position farm under the same variable wind conditions. This effect is on the same scale of yield improvement as other wake management strategies, like wake steering and axial induction control (AIC). The benefits of this technique are highly site-dependent. Sites with bifurcated wind roses show the most benefit. Yield uplift is also highly dependent on allowed frequency of turbine movement - the same bifurcated wind rose sites show up to 2% yield improvement even at low frequency of movement (one excursion per day), while other sites show yield improvement only for high movement frequency (up to 18 excursions daily). CapEx modelling techniques from Velosco Energy, and naval architecture input from Apollo Engineering, were used to investigate the costs of constructing a wind farm capable of dynamic repositioning, for a specific three-line winched mooring design. The costs for this design are roughly double the monetary value of the extra energy produced, showing a lack of financial feasibility. However, there may be other design concepts which are financially feasible.

# Dedication

Thank you to everyone who has helped me throughout this degree, especially my mother, who has sent me across the Atlantic Ocean to study at the University of Edinburgh, supporting me emotionally and financially for such a huge personal and professional transition. Next, thank you to Scott Love and Kutlu Balci at Velosco Energy for their extreme generosity with their time, industry expertise, professional connections, and modelling resources - this dissertation would be far emptier without their support. Thank you also to Dr. Andrew Lyden, my supervisor, who supported me throughout the dissertation process, helping me to find a project which suited me and instructing me on presenting my findings to academia. Thank you to Nigel Robinson and Will Brindley at Apollo Engineering for providing their wealth of naval engineering experience to help me evaluate costs and feasibility of speculative mooring systems. Thank you to my friend and fellow Haverford '23 graduate-turned-postgraduate Jack Crump for supporting me through our journeys as postgraduate academics, and for proofreading my longest-ever academic product (this thesis). Finally, thank you to my MSc Sustainable Energy Systems cohort for their friendship and camaraderie starting in September 2023, through the summer dissertation, and hopefully well into the future.

# Contents

<b>Declaration</b>	i
<b>Abstract</b>	ii
<b>Dedication</b>	iii
<b>List of Figures</b>	vi
<b>List of Tables</b>	ix
<b>Abbreviations</b>	x
<b>Nomenclature</b>	xi
<b>1 Introduction</b>	1
1.1 Motivation . . . . .	1
1.2 Hypothesis . . . . .	3
<b>2 Background and Literature</b>	4
2.1 Floating Offshore Wind . . . . .	4
2.1.1 Resource . . . . .	4
2.1.2 Current State of the Industry . . . . .	8
2.1.3 Design . . . . .	9
2.2 Wind Turbine Wake . . . . .	13
2.2.1 Wake Mechanics . . . . .	13
2.2.2 Turbine-Control Wake Management Strategies . . . . .	15
2.3 Cutting Edge Naval Architecture . . . . .	21
2.3.1 Mooring . . . . .	21
2.3.2 Speculative Motion Options . . . . .	22
<b>3 Methodology</b>	23
3.1 PyWake Simulation . . . . .	23
3.1.1 Farm-Level Wake Deficit Model . . . . .	24
3.2 Financial Feasibility . . . . .	30

3.2.1	EYA Analysis . . . . .	30
3.2.2	CapEx Models . . . . .	31
<b>4</b>	<b>Results</b>	<b>34</b>
4.1	Static Model Performance Analysis . . . . .	34
4.2	Dynamic Model Performance Analysis . . . . .	34
4.2.1	Site Suitability . . . . .	36
4.3	EYA analysis . . . . .	37
4.4	CapEx analysis . . . . .	38
<b>5</b>	<b>Discussion</b>	<b>40</b>
5.1	Future Work . . . . .	40
5.1.1	Input Data . . . . .	40
5.1.2	Implementing Better Wake Models . . . . .	41
5.1.3	Designing Control Schemes . . . . .	41
5.1.4	Modelling Alternative Designs for CapEx and AEP . . . . .	42
5.1.5	Global Site Survey . . . . .	44
5.2	Conclusions . . . . .	45
<b>References</b>		<b>46</b>
<b>A</b>	<b>GitHub: Python and Spreadsheets</b>	<b>52</b>
<b>B</b>	<b>Zotero Library Link</b>	<b>53</b>

# List of Figures

1.1	Two farm layouts (abstracted, not to scale) with two different incoming wind conditions (blue arrows), turbines (blue circles) and their resulting wakes (red arrows). In order from 1 to 4, these layouts represent snapshots of how a dynamically positioned farm can minimize wake losses by repositioning to adapt to instantaneous wind conditions. . . . .	2
2.1	This is an example of a wind rose, which contains six months of time series wind data from the Horns Rev Wind Farm off the coast of Denmark. An ideal wind rose would use a full year's data or multiple years, this plot is constrained by data acquisition costs. This site has very widely distributed wind direction, but frequent high wind speeds. . . . .	5
2.2	These two maps, from [1], show the potential spatial range for bed-fixed offshore wind turbines (top) and floating offshore wind turbines (bottom) in U.S. waters. The maps are color coded according to mean wind speed, where higher wind speeds, and thus greater potential for energy yield, are darker blue, and slower wind speeds are closer to white. It is clear that there is significantly more spacial range and higher wind speeds available to floating offshore. . . . .	7
2.3	This is a schematic of the UMaine 15MW reference platform which features three peripheral semi-submerged buoyant columns arranged in a triangle, with a central fourth column supporting the turbine [2]. . . . .	10
2.4	This figure from [3] shows three distinct platform types used in floating offshore wind; (a) semi-submersible tripod, (b) tension leg platform, (c) spar-buoy. . . . .	10
2.5	From [4], this diagram shows a catenary mooring (left) which uses line (often chain) weight to generate restoring force, and taut leg mooring (right) which uses rope elasticity to generate restoring force. . . . .	11
2.6	Generated with software from [5], this figure shows a 750MW, 50 turbine farm array layout which shows the cable strings that connect FOWTs to the farm OSP. Strings are limited in length by the cables' voltage capacity; too many turbines in series require higher rated cables which become excessively costly. In this instance, five-turbine strings are most cost-effective. . . . .	12

2.7 From [6], this figure shows floating dynamic inter-array cables connecting floating wind platforms. . . . .	13
2.8 From [7], a diagram of the vortex structure in the near wake, where the circles, labelled “ $\Gamma$ ”, represent tip vortices. The vortices propagate/roll downwind in the axial direction, and form a corkscrew shape due to the rotation of the blade and the motion of the tip relative to the airflow. . . . .	14
2.9 From [8], a diagram of the wake structure as a function of axial distance from the turbine. As the vortices lining the wake dissipate the wake expands vertically and crosswind but recovers flow velocity and reduces turbulence intensity at the edges of the wake. . . . .	15
2.10 This wake map is a snapshot of a windfarm as seen from above which was simulated in the course of carrying out the experiment. The intensity of the wake is indicated with darker shades of blue implying slower and more turbulent air. In this particular snapshot, the wakes flow downwind between the turbines for a distance, thus decreasing the effective wake loss. . . . .	16
2.11 This wake map is a snapshot of a windfarm as seen from above which was simulated in the course of carrying out the experiment. The intensity of the wake is indicated with darker shades of blue implying slower and more turbulent air. In this particular snapshot, the wakes flow downwind and directly impact downwind turbines, incurring heavy wake losses. . . . .	16
2.12 From [9], fig. 2.12-A shows the yaw error introduced and resulting wake shift, while fig. 2.12-B shows a wind speed map for a 5-turbine farm without wake steering, and fig. 2.12-C shows the same wind speed map on the same farm with wake steering enabled. . . . .	18
2.13 From [10], this figure shows a variety of mooring topologies and the line weights required/incurred. . . . .	22
3.1 This chart shows methodology flow from the inputs (blue), intermediate processing steps (green), interim outputs (orange,) and goal result (red). . .	23
3.2 From [11], this plot shows the centerline wind speed deficit as a function of distance from the turbine. In the far wake (beyond $\frac{X}{D} = 400$ , the NOJ model has the lowest deficit, and therefore the highest wind speed, least wake effect, and worst hypothetical efficiency boost for a wake management strategy	25
3.3 Wind roses for each of the six sites considered in the study, generated with the author’s data pipeline and PyWake. . . . .	28
3.4 The following are three sequential wake maps of a dynamic farm as it changes over time to maintain optimization in shifting wind conditions. From position 1 through position 4 (over four hours), the wind shifts from ESE to SE, and the turbines slightly adjust position to better accommodate wake effects. Wake intensity is shown by the intensity of blue hue. The right-side figure is the wind rose for the site. . . . .	30

3.5	Sample 2D geometry governing the line lengths of paying-in and paying-out mooring lines. Here, $R$ is the initial anchor radius, $L$ is the initial line length, and $d$ is the water depth. $R + \text{motion range} = R''$ and $L''$ is the longest line length required in the system. In actuality, the 3-Dimensional nature of the problem complicates this geometry, as one of these triangles is set at an angle out of the page, and that angle changes with the motion of the turbine, as is visible from the top view. . . . .	32
4.1	This plot shows the annual AEP gained by having a dynamic farm for each site, under different wind direction sensitivity settings. The most sensitive setting, $1^\circ$ (where the turbines move to a new optimal position if the wind shifts by one degree), yields the highest improvements, while the least sensitive setting, $90^\circ$ , incurs serious penalties on some sites, but remains better than an optimal static farm for other sites. There are small error bars on each plotted bar representing the uncertainty in yield gain obtained via propagation of the uncertainty in wind data. . . . .	35
4.2	This plot shows the average number of movements per day that a turbine at a particular site undertook while operating as a dynamic farm for a variety of wind direction sensitivity settings. . . . .	36
5.1	This image shows a top view of a design concept by Will Brindley for a dynamically positioned wind turbine array using SAL mooring, in which turbines are using yaw misalignment to both thrust into position and to steer wakes away from other turbines in the array [12]. . . . .	44

# List of Tables

2.1	This table, from [13], shows the potential resource for both fixed-bed offshore and floating offshore wind turbines in eight emerging markets, along with observations on the condition of the resource in relation to grid access, regional development, and supply chain. . . . .	8
3.1	Table of relevant characteristics at each of the six sites modelled. . . . .	27
4.1	For each site and direction sensitivity setting, this table presents the associated revenue (USD) and Net Present Value (USD) . . . . .	37
4.2	This table shows calculated cost of line upgrades based on the allowed excursion range and the depth of the water. The maximum allowed depth:excursion ratio was 20:7 on account of naval architecture constraints [12]. . . . .	38
4.3	This table shows the total expected upgrade CapEx to create a dynamic farm, as a function of excursion range, at the minimum allowable depth for these excursion ranges. The winch costs cited here are conservative, and optimistically could cost as little as \$15 million [12]. . . . .	38

# Abbreviations

**AEP** Annual Energy Production.

**AIC** Axial Induction Control.

**AWC** Active Wake Control.

**FOWF** Floating Offshore Wind Farm.

**FOWT** Floating Offshore Wind Turbine.

**GBP** Great British Pound, currency.

**IAC** Inter-array Cable.

**NOJ** Neils Otto Jensen.

**TSR** Tip Speed Ratio,  $\lambda$ .

**USD** United States Dollars, currency.

# Nomenclature

Term	Description	Units
Axial Induction Factor	$\alpha$ , The fractional difference between free stream wind velocity and the wind velocity at the rotor. This factor relates to the amount of power extracted from the wind.	unitless
CapEx	Abbrev. Capital Expenditure, the initial installation, construction, labor, and materials cost of a farm or turbine, but not the future maintenance or operational costs.	<i>GBP, USD, as applicable</i>
CFD	Abbrev. Computational Fluid Dynamics (not to be confused with CfD, Contracts for Difference) is a broad term referring to methods of generating detailed simulations of aerodynamic effects [on or by wind turbines].	—
CfD	Abbrev. Contracts for Difference ( not to be confused with CFD, computational Fluid Dynamics) are contracts offered by the UK National Grid Electricity System Operator where a generator is guaranteed a "strike price" for generated electricity for the duration of the contract - if the grid price exceeds the strike price, the generator pays revenue back to the grid operator, but if the grid price is below the strike price, the generator still receives the full revenue from their sales at the promised strike price. Strike prices can be set well above expected grid prices in order to subsidise investment in renewable energy, and this is especially true for fixed-bed and floating offshore wind farms.	—

Term	Description	Units
Dynamic Farm	A floating offshore wind farm with the capability to move its platforms in response to changing wind conditions. Used interchangeably with "moving farm" or "breathing farm". A dynamic farm must be modelled with a time series of wind speed and direction data, rather than a Weibull Distribution.	—
Excursion	A word which describes a departure from the central/intended position of a FOWT on the surface of the ocean. Excursions can be intended or allowed, or they may be unintentional or dangerous to turbines or surrounding infrastructure. In this thesis, excursion can refer to both natural movement in "static" floating farms, as well as extreme or powered platform movement in "dynamic" floating farms.	—
$H_\infty$	A control algorithm used to control operational set points like blade pitch angle, such that the set point can rapidly, but smoothly adjust to new conditions, without overshooting an new optimal set point. Whereas PID and LQI work with the differences between current state and desired state, $H_\infty$ infinity uses a complex and high computation cost optimization matrix to find control values to reach the desired state.	—
LQI	Abbrev. Linear-Quadratic-Integral, a control algorithm used to control operational set points like blade pitch angle, such that the set point can rapidly, but smoothly adjust to new conditions, without overshooting an new optimal set point. Whereas PID focuses on linear models, LQI adds an integral term to LQR (Linear Quadratic Regulator) controls which focus on systems with nonlinear models.	—
NOJ	Neils Otto Jensen's eponymous simple Wake-Deficit Model [14].	—
NPV	Abbrev. Net Present Value, The sum of all future cashflows (after a discount rate is applied) within the planned lifetime of a wind farm, less the investment responsible for those cashflows	<i>GBP, USD, as applicable</i>

---

<b>Term</b>	<b>Description</b>	<b>Units</b>
OpEx	Abbrev. Operational Expenditure, sometimes synonymous with O&M, or Operations and Maintenance. This term refers to the costs associated with operating an asset which are not tied to the initial investment. In this case, that would include costs associated with inspections, maintenance, marine vessels required to carry out other operations tasks, etc. OpEx is not investigated or quantified in this study, but is considered as a design constraint in the discussion in Ch. 5.	<i>GBP, USD, as applicable</i>
PID	Abbrev. Proportional-Integral-Derivative, a control algorithm used widely in the wind industry to control operational set points like blade pitch angle, such that the set point can rapidly, but smoothly adjust to new conditions, without overshooting an new optimal set point.	—
Static Farm	A floating offshore wind farm without the capability for directed movement.	—

# Chapter 1

## Introduction

### 1.1 Motivation

Floating offshore wind turbines are likely to be a major component of the future global energy mix. Offshore wind turbines are useful as they avoid taking up land space and dealing with onshore regulation, residences, and infrastructure. Offshore wind turbines often have access to faster, higher altitude winds, which are also less turbulent. However, there is relatively little space for fixed-bed offshore wind turbines, which make up the majority of current commercial offshore wind generation, as these turbines require shallow waters ( $\leq 60\text{m}$ )[15]; the potential wind resource which is exclusively available to floating offshore wind farms is enormous [16].

However, there are many challenges in building and operating floating offshore wind turbines. No matter what sort of turbine, all wind turbines situated in arrays suffer from some wake losses. As turbines extract energy from the wind, they disturb the flow of air downwind, creating a wake. Directly incident wakes can reduce the energy yields of a downwind turbine by up to 40% [9][17], particularly in the second row of turbines in an array, which receive the most fractionally disturbed airflow, but get the least benefit from the remixing of wakes. Across an entire farm, power losses due to wake average to around 10% [18], with onshore farms observing roughly 8% loss, and offshore farms observing a more significant 12% loss [19]. Because wakes locally affect turbines directly downwind from them, wind conditions and the orientation of rows of turbines within a farm are important factors in the ultimate yield of a farm [20]. Typically, this means that array designers will attempt to create farm layouts which - for a given site with a set of historical wind data - will allow the wakes to pass between turbines, rather than hitting them directly, as in figures 1.1-2 and 1.1-4. Additionally, wakes increase the turbulence intensity of outflow wind, which increases fatigue loads on downwind turbines by 5-15% and reduces turbine operational lifespans [21]. As such, wake effects on energy yield are rightfully a significant design consideration for wind energy systems.

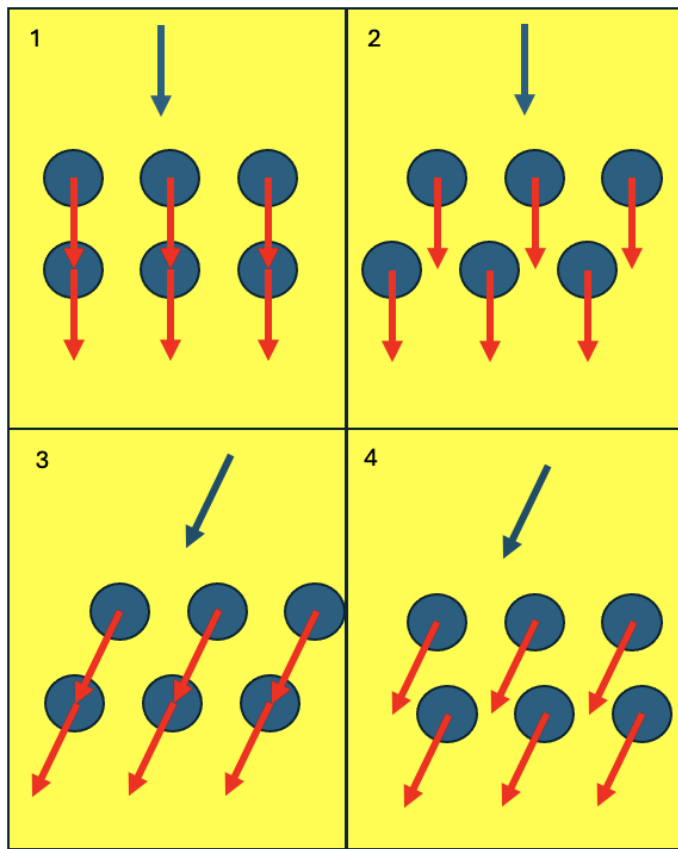


Figure 1.1: Two farm layouts (abstracted, not to scale) with two different incoming wind conditions (blue arrows), turbines (blue circles) and their resulting wakes (red arrows). In order from 1 to 4, these layouts represent snapshots of how a dynamically positioned farm can minimize wake losses by repositioning to adapt to instantaneous wind conditions.

There are several existing methods for reducing energy yield losses due to wakes, including wake steering and axial induction control (AIC). The simplest is designing arrays which sacrifice space efficiency and cable cost efficiency to allow for increased spacing between turbines; increasing the space between turbines allows wakes more time to dissipate before they hit a downwind turbine, thereby reducing the wake-derived power losses. There are also at least three distinct wake management strategies that rely on turbine control schemes [17], which will be examined in Chapter 2. Implementation of wake management practices, can increase annual energy production by a few percent. This may seem small, but a 1% increase in capacity factor across 500 GW of wind energy can be worth up to 850 million USD per year [17]. In 2023, global wind capacity was estimated at 906 GW, with projections for 1500 GW by 2028 [22], so wake management can result in significant annual economic upside across the industry. Generally, existing wake management strategies are able to achieve about a 1-3% increase in AEP and capacity factor across large farms in realistic scenarios. That improvement can be closer to 15% for special cases, like two-row arrays in specific wind conditions [23] or very small or unoptimized arrays. All of the existing methods for wake management are therefore quite valuable for on-shore and fixed-bottom wind farms. However, all existing strategies are only able to slightly modify wakes, rather than avoid their

affects altogether.

The motivation for this thesis is to probe the distant future of wake management strategies, particularly for FOWTs, on which wakes incur greater losses than on onshore turbines due to a lack of turbulence and a lower planetary boundary layer height, two factors which help to remix the wakes of onshore turbines [24]. So, FOWTs suffer serious wake losses and are subject to very different design constraints from their fixed-bed counterparts, but may also have unexploited design features. Namely, FOWTs have some capability to move across the ocean surface. Typically, FOWTs are subject to "station keeping" in a very small (20-50 meter diameter) predetermined area by their mooring systems, which have some slack to help the FOWT platform better handle wave and current loads in the chaotic marine environment. This study aims to assess the wake management capabilities FOWTs offer, given a mooring system whereby turbines can reposition themselves outside of upwind wakes (as in fig. 1.1). This study also endeavors to characterize the wind conditions that are best suited to dynamic FOWFs. Further, this thesis seeks to question industry experts and academic literature to find technologies and designs which could support the movement capabilities of these FOWTs. Lastly, and with the help of these industry experts, this study aims to calculate the economic feasibility, advantage, or disadvantage of implementing dynamic FOWFs, analysis which has been sparse in the wider literature.

## 1.2 Hypothesis

Because a dynamically positioned FOWT array is able to adapt to instantaneous wind conditions to better optimize against wake and maximize power output, a simulated dynamic FOWF will show significant energy yield increases (at least on the same scale of other wake-management strategies). Further, it is hypothesized that energy yield improvements due to dynamic positioning will not be economically feasible in the short to medium term due to underdeveloped mooring and positioning technology. However, in the long term, particularly as technology improves and space constraints become more significant for marine energy systems planning, dynamically positioned FOWFs will be economically advantageous for certain wind sites.

# **Chapter 2**

## **Background and Literature**

### **2.1 Floating Offshore Wind**

This first section discusses the broad context of floating offshore wind turbines (FOWTs). Floating offshore wind is a relatively new and immature technology, as it combines all of the engineering challenges of a normal wind turbine with the logistical challenges of working in harsh marine environments, and the loading challenges that come with large wind and wave forces incident on a platform only flexibly anchored to a solid seabed. The benefits of floating offshore wind could be enormous however: fixed bottom wind turbines require or are only financially viable in shallow water ( $\leq 60$  meters)[\[15\]](#), which severely constrains siting options. Winds are steadier, with higher average speeds over the ocean, which is useful for increasing both power and capacity factor of wind farms, driving farms further and further offshore and building demand for turbines in deep waters [\[25\]](#). FOWT therefore have significantly more siting options than fixed bed turbines, and therefore more potential to contribute to the global energy mix and decarbonize energy systems.

Floating offshore turbines may be friendlier to sensitive marine environments than bottom-fixed turbines. Pile driving is one of the most environmentally damaging elements of creating an offshore wind turbine as it is destructive to the ocean floor and emits particularly loud noise. Pile driving injures, disrupts, displaces, and changes the behavior of marine mammals and fish species [\[26\]](#). Pile driving is necessary to construct the foundations for bottom fixed turbines, but FOWTs typically do not require pile-driven foundations. Of course, FOWTs also come with greater weather damage and failure risks, higher costs, additional logistical/maintenance challenges, and higher investment cost (CapEx) and leveled cost of energy (LCOE). Some of these risks and costs may be reduced as the technology develops, though remote floating turbine sites will always be difficult to service and somewhat more susceptible to extreme weather.

#### **2.1.1 Resource**

Wind turbines convert kinetic energy and momentum in the wind to electrical energy and momentum in the turbine blades - the wind energy that a turbine receives therefore deter-

mines, in part, how productive a turbine will be. The wind energy resource of a site can be measured as an electrical figure given an average wind speeds and turbulence intensity for the site, which is converted to an electrical power according to the wind speed vs. power plot (called the “power curve”) of a standard model turbine, such as the NREL 15MW turbine design. The power estimate can be converted to an energy estimate by taking the time integral of the power. Wind speed is therefore important to characterize when measuring the available resource; similarly, characterizing wind direction is crucial to planning an actual wind farm, as the farm’s layout must be optimized for the direction of the wind. Wind directions are characterized by a “wind rose” plot, which sorts a year’s worth of wind-speed and direction data into a compass plot, indicating the frequency, speed, and direction of the wind. A sample wind rose can be found in fig 2.1 and a further six example wind roses are shown in fig. 3.3, where plot area represents frequency (as a fraction of the data period), color represents wind speed, and the position on the compass represents wind direction.

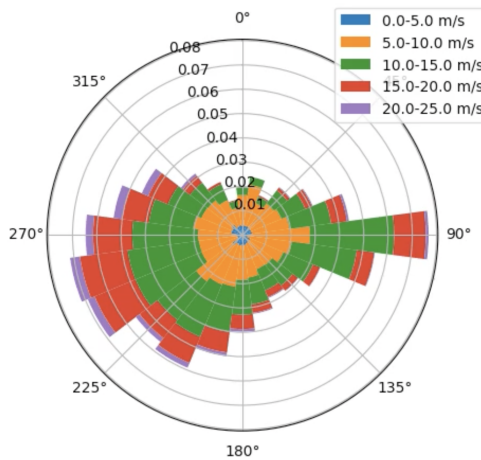


Figure 2.1: This is an example of a wind rose, which contains six months of time series wind data from the Horns Rev Wind Farm off the coast of Denmark. An ideal wind rose would use a full year’s data or multiple years, this plot is constrained by data acquisition costs. This site has very widely distributed wind direction, but frequent high wind speeds.

Given that FOWTs sit on the oceans’ surface, which cover more than 2/3 of the Earth’s surface, it’s challenging to count the total resource which might be available to floating offshore turbines. However, even floating turbines are subject to siting constraints – turbines must be close enough to shore to transmit electricity back to shore, they must not obstruct shipping lanes or other essential ocean activities, they should avoid interfering with ecosystems, and they’re often not welcome sights for beach communities, which can present a serious obstacle to constructing FOWFs [1]. The greatest limitation to viable floating offshore wind is that FOWFs have maximum water depths, which get larger as technology improves, but currently sits around 1000 meters [13], which, in combination with the shore proximity limitations, eliminates most of the ocean as viable sites for FOWFs. Wherever fixed-bottom turbines are viable ( $\leq$  60 meter water depths) these will usually take precedence over FOWTs, on the basis of economic and operational efficiency. One study from the

(U.S.) National Renewable Energy Lab (NREL) endeavored to find the resource potential within U.S. territorial waters. The study collected information on all off-shore area within the U.S. jurisdiction, including the Great Lakes, then filtered the areas according to siting constraints, then estimated the resource based on wind data. They found that there were approximately 1.5TW of resource capacity, or roughly 4.6 petawatt-hours per annum of generation (which would imply a capacity factor of roughly 35%) for *fixed bottom offshore wind* and 2.8TW of resource capacity, and 9PWh of energy per annum for *floating offshore wind* [1]. Fig. 2.2 shows two maps of sites in U.S. territorial waters that are viable for offshore wind, split between bed-fixed and floating.

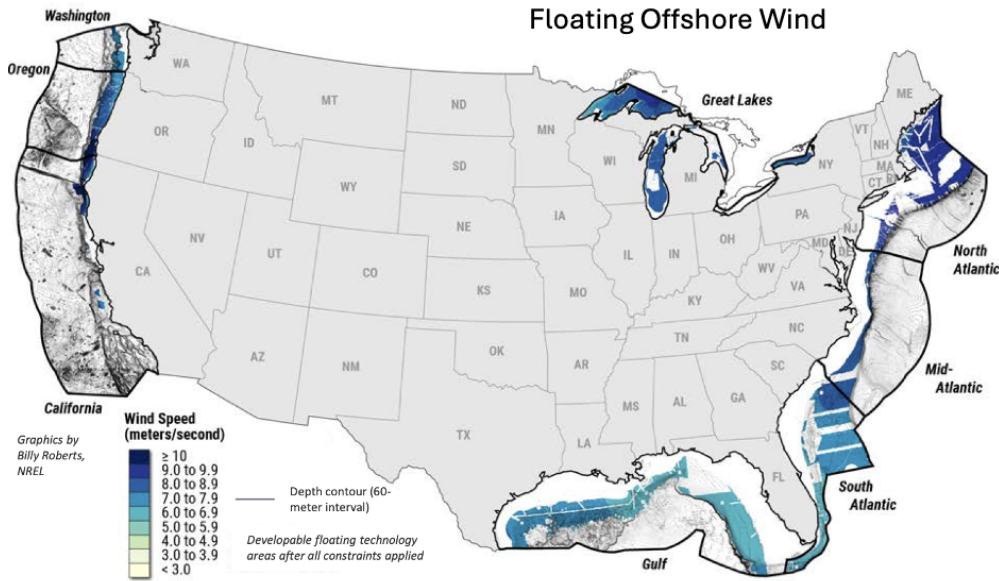
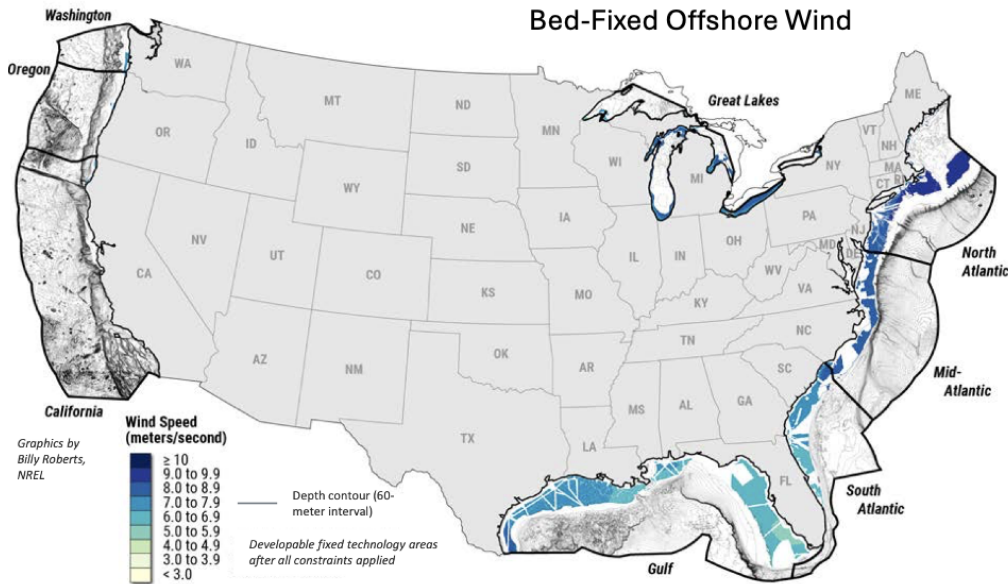


Figure 2.2: These two maps, from [1], show the potential spatial range for bed-fixed offshore wind turbines (top) and floating offshore wind turbines (bottom) in U.S. waters. The maps are color coded according to mean wind speed, where higher wind speeds, and thus greater potential for energy yield, are darker blue, and slower wind speeds are closer to white. It is clear that there is significantly more spacial range and higher wind speeds available to floating offshore.

A World Bank report of technical resource potential (the resource which is extractable with current technology, not which is actually likely to be exploited) found that there were 2TW of resource capacity across just eight coastal emerging markets, including Brazil, India, Morocco, the Philippines, South Africa, Sri Lanka, Turkey and Vietnam, again nearly double the resource for bottom fixed turbines [13]. For some of these countries, the proportion of

resource which was exclusively available to floating turbines was 10x that which was available to fixed bottom wind turbines, indicating that, in these emerging markets, floating offshore wind may be the key to unlocking high capacity renewable energy. An influx of renewable energy to these countries would be particularly impactful for global decarbonization as these are, generally speaking, highly carbon-intensive countries, in the process of grid modernization and industrial transition. A full breakdown of the resource potential for these markets can be found in table 2.1.

Table 2.1: This table, from [13], shows the potential resource for both fixed-bed offshore and floating offshore wind turbines in eight emerging markets, along with observations on the condition of the resource in relation to grid access, regional development, and supply chain.

Country	RISE Score	Potential GW		Observations
		Fixed	Floating	
Brazil	71	480	748	Brazil has excellent potential with shallow waters close to demand centers and a strong supply chain potential.
India	87	112	83	Set an offshore wind target of 5 GW by 2022 and 30 GW by 2030. Best opportunities are in Tamil Nadu and Gujarat.
Morocco	67	22	178	Excellent wind speeds and suitable depths along the Atlantic Coast; regional synergy possible with Spain and Portugal.
Philippines	62	18	160	Best potential in the north and central areas; potentially synergies with regional development (Taiwan, Vietnam).
South Africa	76	57	589	High wind speeds but deep waters will favor floating foundations. Few regional development synergies likely.
Sri Lanka	55	55	37	Strong winds and shallow waters suggest potential for fixed foundation. But limited power demand affects scalability.
Turkey	75	12	57	Good winds but deeper waters may favor floating; key issues around shipping and proximity to demand.
Vietnam	67	261	214	Excellent resource off southwest coast; existing nearshore development; strong potential for floating and fixed.
<b>Totals</b>		<b>1,016</b>	<b>2,066</b>	<b>Grand Total = 3,082 GW</b>

Globally, the World Bank Group estimates there is 10.7TW of technical potential capacity across its member states (the entire world excluding Andorra, Cuba, Liechtenstein, Monaco, North Korea, Palestine, and Taiwan) [27]. Of course, only a small fraction of this actually *will* be extracted, subject to energy policy, investment, and consenting, but it highlights that floating offshore wind is likely to fill a much larger proportion of energy demands in the future.

### 2.1.2 Current State of the Industry

As of 2018, only 50MW of floating wind turbine capacity had been installed globally [15]. Just five years later, in 2023, there were at least 227MW installed globally, spanning fourteen projects in seven countries; after Norway with 94MW in three projects, the UK has the second most installed capacity, with 80MW of floating offshore wind. The current global project pipeline (which includes any project from an early development stage to fully operational projects) has grown to nearly 250GW. In addition to the 2023 count of 227MW, 46MW are currently under construction over three projects, with an additional 576MW in a committed, consented, pre-construction planning phase, representing eleven projects. A further 68GW

(300x the current installed capacity) representing just eighty projects are in planning or have a lease agreement [28] - the growth in scale of individual projects is accelerating, rapidly. This indicates that increasing installation of floating offshore wind is bolstering installation experience and confidence is growing in floating offshore wind as a viable route for affordable and reliable renewable energy. The growing scale of projects also highlights the need for further study into inter- and intra-array aerodynamic interaction, like wake effects. Still, a vast majority of the capacity in this pipeline is speculative, and faces serious policy, funding, and execution hurdles. However, if even a fraction of the project pipeline is constructed, the world will see a huge influx of offshore renewable energy. This influx will maximally decarbonize global energy systems only if the offshore technologies being deployed are reliable, optimally efficient, and ecologically friendly - it is immediately important to determine which systems are capable of reliability, efficiency, and ecological safety.

### 2.1.3 Design

As a nascent category of wind turbine, with significantly different design constraints, there is significantly more variation in design for FOWTs than amongst the more-or-less converged designs that are used for onshore or bed-fixed turbines. Still, the windmill elements of FOWTs are similar or identical to bed-fixed offshore designs; most of the design variations for FOWT occur in the floating platform or mooring system. These systems are focused primarily on dampening the wave reaction motion of a semi-submersible floating platform or in achieving specific mooring aims which might collectively improve the efficiency of a floating turbine or reduce loads, vibration, and fatigue.

#### Platform Design

The most commonly seen type of semi-submersible platform is a set of three buoyant columns, arranged in an equilateral triangle. Turbines often sit on a fourth column which sits in the middle of the triangle as is seen in the UMaine 15MW reference platform [2], which can be seen in fig. 2.3. Alternatively, turbines may sit on a side or a vertex of the triangle to create a weathervaning platform which rotates to support specific yaw behavior under wind or wave conditions [29]. Turbines may less commonly have other floater structures such as a tension leg platform (in which the entire platform is submerged) or spar-buoy (for which the turbine is mounted on a single semi-submerged column floater) [3] as seen in fig. 2.4. Other, more experimental, designs include the Ideol damping pool, which uses a central pool enclosed within the buoyant walls of a rectangular floater to effectively behave as a mass-spring damping system [30], or three-column V-shaped floaters which are flexible to oncoming waves in order to damp turbine motion [31].

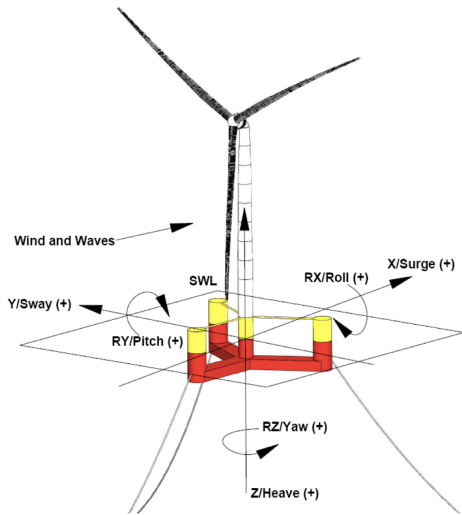


Figure 2.3: This is a schematic of the UMaine 15MW reference platform which features three peripheral semi-submerged buoyant columns arranged in a triangle, with a central fourth column supporting the turbine [2].

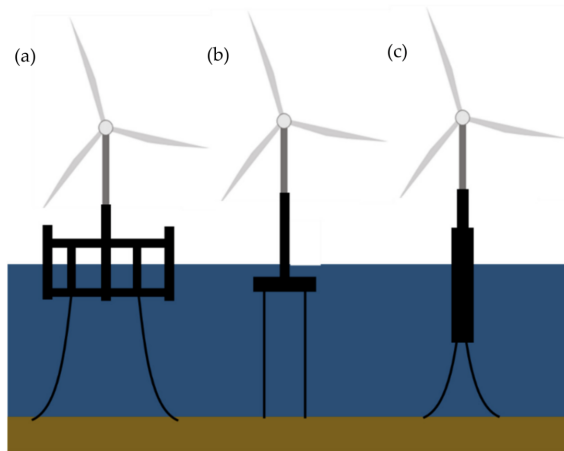


Figure 2.4: This figure from [3] shows three distinct platform types used in floating offshore wind; (a) semi-submersible tripod, (b) tension leg platform, (c) spar-buoy.

## Mooring Design

Floating wind turbines are expensive, and it is technically and financially challenging to secure these assets by mooring them to the seafloor. The ocean is a harsh environment; floating turbines and their anchoring systems undergo huge wind and wave forces [32]. As such, mooring is considered a priority target area for innovation by industry research groups [15]. Thanks in part to expertise from the oil and gas industry, there are a number of well developed mooring systems, which may be used to secure offshore floating wind turbines. The two main categories are catenary mooring systems and taut leg mooring systems. These systems are pictured in fig. 2.5. Catenary moorings allow significant slack, such that long sections of mooring line lay on the seabed; the self-weight of the mooring line (often chain) thus acts as a restoring force transmitted along the line as tension. Taut leg mooring systems which

use taut lines from anchor to platform, and feature narrower anchor spread, but allow less dynamic response, which arises mostly from the stretch of the line [4].

Synthetic fiber ropes are increasingly used by floating renewable energy platforms, especially as depths increase, because they have lower weight (weight is not useful in a taut leg system) and cost. Synthetic fiber ropes have more complex behavior than chains or wire rope, as they have a non-linear, load-path dependent, change-in-length response to loads, which can be challenging to model and predict in complex marine loading environments. Industrial standard practice is to establish an upper and lower bound of the loads on and tensions exerted and sustained by these ropes and design within that envelope [33]. Taut leg mooring is therefore more suitable for deep and ultradeep water applications, thanks to its advantage when it comes to anchor spread; FOWFs would require extreme spacing between turbines for catenary moorings to remain untangled in deep and ultradeep waters. Deep waters also work well for taut leg moorings as more depth allows more length of taut line, and therefore more predictable response and more absolute response from the stretch of the line. For the same depth, taut lines will always be shorter than catenary lines, and therefore taut leg moorings are much cheaper than catenary moorings in deep waters.

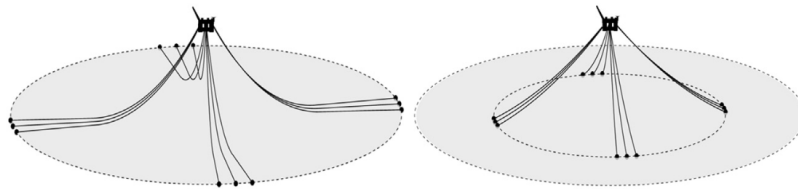


Figure 2.5: From [4], this diagram shows a catenary mooring (left) which uses line (often chain) weight to generate restoring force, and taut leg mooring (right) which uses rope elasticity to generate restoring force.

There are many further categorizations of mooring systems, but an important one for this discussion are disconnectable moorings - across industries, disconnect capabilities of permanent moorings are used for safety as they allow moored structures to be moved in instances of extreme weather without needing to re-lay a mooring system when the structures return [4]. Disconnectable moorings are also making an entrance to offshore floating wind, with the debut of designs like the PALM Quick Connection System, which is being developed as a cost-competitive mooring system to which wind turbines can be quickly connected and disconnected for installation and maintenance [34].

### Cable

While cables are perceived to be a simple and established technology, they're actually considered a priority target area for innovation by industry research groups [15] on account of anticipation that increasingly large quantities of energy will be flowing from increasingly large turbines which are increasingly far from each other and the shore. While bottom-fixed turbines are in shallow enough water to install bottom-fixed cables, floating turbines must

connect to an offshore substation platform (OSP) with free-floating cables for at least part of the length of the electrical connection. Cable which floats in water column, either in order to reach bed-fixed cables or another floating structure are called dynamic cables. Dynamic cables can be very capital intensive as they contain large amounts of metals (copper) and shielding, and must also be resistant to damage from motion due to wave and current forces - for this reason, dynamic cable often sits within the water column, supported and weighted by alternating positively and negatively buoyant “buoyancy modules”, rather than floating at the surface [35].

Turbines are connected in strings to an OSP, cable diameters are largest near an OSP to accommodate greater voltages (turbines are connected in series) and smallest at the turbines geographically furthest from the OSP, to save on material costs where just a single turbine is generating. A plot of how turbines might be connected to an OSP is included as fig. 2.6, and a schematic of floating dynamic cable is included as fig. 2.7 It's worth noting that while cable can be very expensive, it's typically less expensive than mooring systems, which operate with many of the same array layout cost variables as cable - cheaper, more relaxed mooring systems at the cost of more expensive cables (designed to withstand higher movement loads) may lead to better cost savings overall [35], therefore motivating further development of robust dynamic cable to enable FOWF.

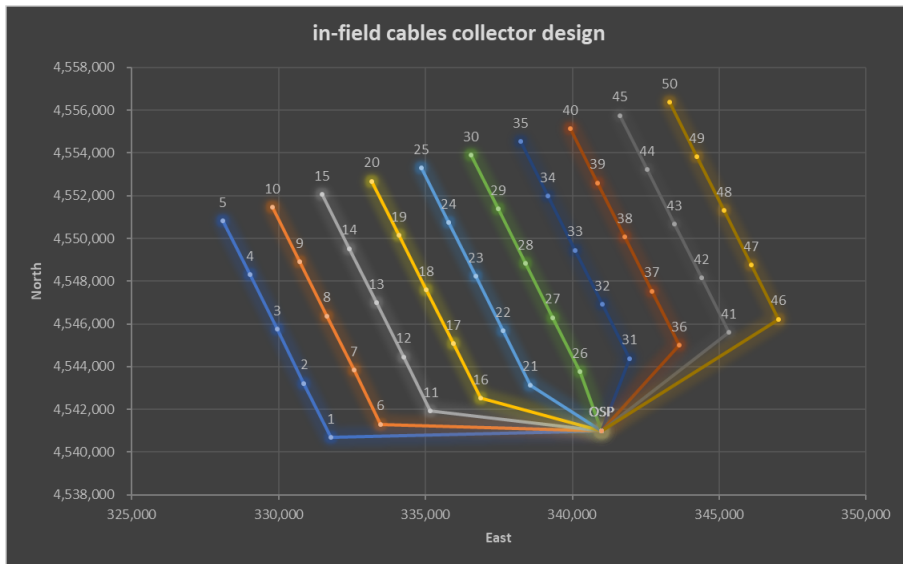


Figure 2.6: Generated with software from [5], this figure shows a 750MW, 50 turbine farm array layout which shows the cable strings that connect FOWTs to the farm OSP. Strings are limited in length by the cables' voltage capacity; too many turbines in series require higher rated cables which become excessively costly. In this instance, five-turbine strings are most cost-effective.



Figure 2.7: From [6], this figure shows floating dynamic inter-array cables connecting floating wind platforms.

## 2.2 Wind Turbine Wake

Wind turbine wakes are serious obstacles to optimal efficiency in wind turbines. This section discusses the governing mechanics of wakes, as well as current and speculative wake management strategies.

### 2.2.1 Wake Mechanics

Wind turbine wakes are the aerodynamic consequences of the motion of the rotor blades - especially the blade tips - and the extraction of energy and momentum from the free flowing wind. At their worst, wakes can reduce turbine power output by 40% [19], but on average over a farm, wakes will reduce output by 10% [17]. This mitigation in loss occurs because, typically some turbines in a farm will not be waked. Additionally, wake losses only affect turbines for wind speeds between cut-in and just greater than the rated wind speed. With great enough inflow wind speed, even wake affected wind has greater velocity than the turbines' rated wind speed, so no power is lost. Effectively, wakes (as averaged over a long period of time) shift the power curve of a turbine to the right on the wind speed axis. When discussing the mechanics that determine the behavior of a wake, there are two main regions of a wake which have separate behavior and are governed by separate mechanics: the near wake and the far wake.

#### Near Wake

The near wake, which extends behind a turbine for a distance roughly one to two rotor diameters (1D to 2D) from the turbine, is driven by turbine geometry and motion, especially at the roots and tips of the blades where the velocity gradient between the oncoming wind, the rotor element itself, and the outflow wind is most extreme [19]. The tip speed ratio (TSR,  $\lambda$ ) for offshore turbines can be as high as 7 or 8, indicating that the tip of the blade

moves through the air 7 to 8 times faster than the inflow wind velocity. The rapid motion of the blade tip generates a vortex as low pressure zones on the trailing edge and back side of the blade suck air in from the high pressure zones on the front surface and leading edge of the blade, as in the smaller circles in fig. 2.8. At high  $\lambda$ , the vortices combine into a continuous shear layer, where the airflow velocity outside the vortices is disjoint from the airspeed within the vortices (the space contained by the shear layer) [19]. The turbine converts momentum and energy from the airflow into electricity, which results in a pressure gradient along the axis of the turbine, which is strongest across the rotor disk. This gradient slows the velocity of the air directly behind the turbine; this loss of velocity is called the wake deficit. Blade roots, where the blade connects to the hub and nacelle of the turbine can also generate strong vortices on account of being the terminus of the blade edges; root vortices are typically dissipated by the aerodynamic effects of the hub, nacelle, and support tower, and are not typically considered significant components of wake losses [36].

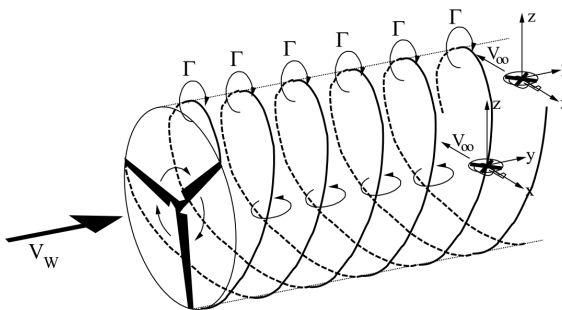


Figure 2.8: From [7], a diagram of the vortex structure in the near wake, where the circles, labelled “ $\Gamma$ ”, represent tip vortices. The vortices propagate/roll downwind in the axial direction, and form a corkscrew shape due to the rotation of the blade and the motion of the tip relative to the airflow.

### **Far Wake**

The far wake is the region of observed reduction airflow velocity which is not directly affected by the motion and geometry of the turbine, and extends from the end of the near wake. In the far wake, turbulence dominates, rather than vortices, and acts to mix the wake back into the free flowing atmosphere. Turbulence in the far wake has three sources, atmospheric turbulence, mechanical turbulence from the turbine, and wake turbulence arising from the breakdown of tip vortices [19]. The mixing effect of this turbulence eventually leads to the average partial recovery of airflow velocity far downstream, leaving a small magnitude, Gaussian, axisymmetric velocity deficit, as in fig. 2.9; industry standards often recommend spacing downwind rows of turbines by seven rotor diameter’s (7D) distance, by which point the wake has remixed enough that further separation between turbines costs more in land usage than it gains in wake recovery benefits.

Wakes typically extend directly downwind from the turbine that creates them, but they expand vertically and crosswind, again, due to tip vortex breakdown turbulence as in 2.9. Depending on the turbulence of the incoming airflow and the tip vortices, wakes can also

propagate in a meandering fashion wherein the wake shifts along the crosswind axis as it travels downwind. There are a variety of models for wakes, ranging from simple, static 2-D numerical approximations [11] that are efficient with computational resources to deep, volumetric mesh simulations that combine techniques from Blade Element Momentum theory, Large Eddy Simulation, and 3-D meandering wakes [19] that require significant computational investment.

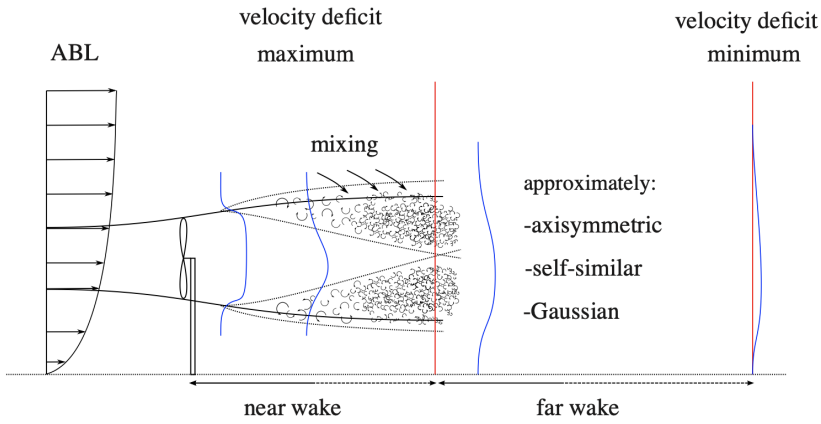


Figure 2.9: From [8], a diagram of the wake structure as a function of axial distance from the turbine. As the vortices lining the wake dissipate the wake expands vertically and crosswind but recovers flow velocity and reduces turbulence intensity at the edges of the wake.

### 2.2.2 Turbine-Control Wake Management Strategies

Wakes are relevant to this study because they reduce turbine power and energy yield while increasing turbulence intensity and fatigue loads (which in turn reduces the lifespan turbines). In order to reduce these effects of wakes, farm designers can increase inter-turbine spacing or shift their array designs to allow wakes to pass between turbines, as is seen in fig. 2.10. However, the former is less space-efficient, and the later is not fully reliable in dynamic wind conditions; if winds shift, the array could find itself suffering heavy wake losses, as in fig. 2.11. Therefore, there are at least three distinct wake management strategies that rely on turbine controls rather than array design and siting constraints, two of which are currently implemented at scale in current farms. There is also some research on strategies that could be considered dynamic positioning, the experimental topic of this thesis.

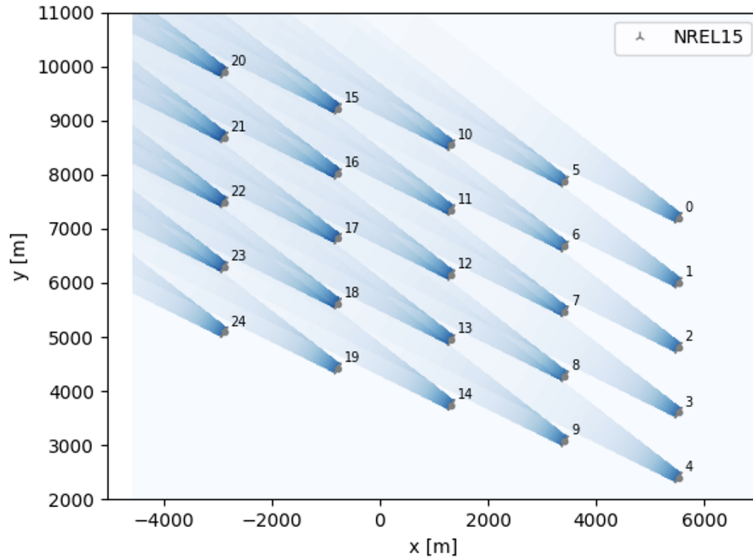


Figure 2.10: This wake map is a snapshot of a windfarm as seen from above which was simulated in the course of carrying out the experiment. The intensity of the wake is indicated with darker shades of blue implying slower and more turbulent air. In this particular snapshot, the wakes flow downwind between the turbines for a distance, thus decreasing the effective wake loss.

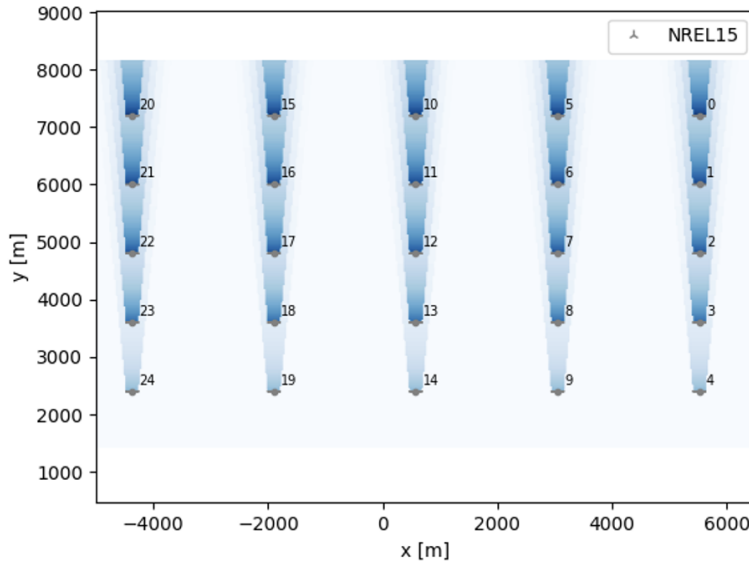


Figure 2.11: This wake map is a snapshot of a windfarm as seen from above which was simulated in the course of carrying out the experiment. The intensity of the wake is indicated with darker shades of blue implying slower and more turbulent air. In this particular snapshot, the wakes flow downwind and directly impact downwind turbines, incurring heavy wake losses.

### Axial Induction Control

The first control-based wake management strategy is axial induction control (AIC), whereby the axial induction factor,  $\alpha$ , (which is related to the power output of a turbine) of individual turbines is adjusted by modifying the tip speed ratio ( $\lambda$ ) and pitch angle [37]. This has the joint effect of reducing power output, blade loads, thrust, and by extension, wake. By creating control algorithms that manage wake via axial induction control, farm-level power output can be increased, even as turbine-level power output is reduced for some turbines in an array [37][38]. Farms which optimize each turbine individually, without reference to the power output of any other turbine are called "greedy". Controlling or derating turbines with AIC can lead to farm-level AEP benefits of around 1%, and can extend farm lifespans by 1.46% compared to greedy farms [17]. This strategy has been implemented and tested in existing wind farms, notably including the Lillgrund offshore wind farm near Copenhagen [39].

### Wake Steering

Wakes may also be managed by introducing yaw error to turbines to "steer" wakes away from other nearby turbines as shown in figure 2.12,[9]. This steering method was shown to increase power production by 7% for small arrays of six turbines, which also demonstrated benefits to farm reliability as a base energy supply [9]. Somewhat counter-intuitively, yawing to the right of the incoming flow direction will also steer the wake to the right of the incoming flow angle, as in 2.12. This is on account of Newton's third law, as yawing the turbine to the right causes a blade thrust in the axial direction (offset to the *left* of the incoming wind direction, due to the yaw) which must then impart a force on the air to the right, relative to the incoming wind direction [17]. Effective wake steering requires significantly more yaw angle than the actual output deflection of the wake that is achieved. With a 30° yaw misalignment and a 4° pitch reduction (to increase thrust on the turbine, which in turn accomplishes greater deflection), one simulation study was able to deflect wake enough to achieve 15% gain in energy yield at the farm-level (relative to a typical 5% gain for strategies modifying only the yaw angle), despite the misalignment power losses on the front row of turbines [23]. This result shows that combining wake management strategies - in this case axial induction control with wake steering - is possible and likely very effective. However, it's worth noting that this study used just two rows of turbines, and that the average affect across a more realistic farm with more rows is likely to be more muted. It does not appear that wake steering has been implemented in full scale offshore farms, thought it has been tested at scale since at least 2017 [40], and implemented in full scale onshore farms since at least 2023 [41].

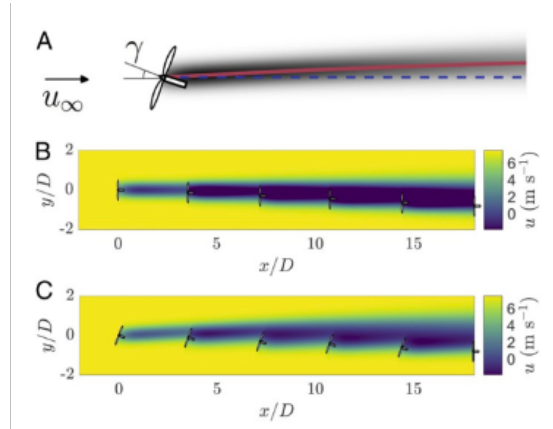


Figure 2.12: From [9], fig. 2.12-A shows the yaw error introduced and resulting wake shift, while fig. 2.12-B shows a wind speed map for a 5-turbine farm without wake steering, and fig. 2.12-C shows the same wind speed map on the same farm with wake steering enabled.

### Active Wake Control

Finally, there is active wake control (AWC), which constantly changes the operating conditions of a turbine (operational setpoints including those for yaw,  $\alpha$ , pitch,  $\lambda$ , and others which might affect the aerodynamic performance of the rotor) in a variety of ways which causes the wake to dissipate faster [17]. This could include using dynamic individual pitch control to steer the wake in a time-varying helix (in much smaller magnitude than in actual wake steering), or adding turbulence to the wake by varying the induction factor continuously. It seems that the most effective frequencies of these adjustments to wake production may be related to some structural instability of the wake, which has become a topic of focus in the field. The highest reported efficiency gain was 3% as compared to non-AWC, for a farm of aligned (and thus wake-affected) turbines. AWC may be able to significantly shorten the near wake region, which could be useful in reducing the required spacing between turbines. These methods are apparently the least studied and most recent/speculative (all tests within the last 7 years). AWC has seen no implementation in full-scale turbines; outside of a few wind-tunnel tests, most studies of AWC are performed as CFD simulations [17].

### Dynamic Positioning

Dynamic positioning, is the experimental topic of this thesis. It consists of moving turbines within an array to react to changing wind conditions, to prevent or minimize the direct incidence of an upwind wake on a downwind turbine, as visualized in fig. 1.1. Dynamic positioning is a strategy which has been conceived of since at least 2014 and studied abstractly since 2015 [25]. Modeling of a dynamic positioning scenarios has been conducted in some limited format (10-15 m excursion range), since at least 2017 [42]. Rodrigues et al. (2015) present the first study on how to design a farm composed of movable floating turbines, and compared efficiencies at excursion ranges for a variety of wake models [25]. In simulations, they observed up to 4.4% greater wind farm efficiencies, particularly with

large excursion ranges. Kheirabadi et al. (2019) consider repositionable turbines that control movement aerodynamically through yaw misalignment and induction control, with up to 925 meter catenary mooring lines that yield crosswind displacements up 69.9 meters. The thrust generated by wind incident upon the rotor plane in the downwind axial direction is thus controllable in magnitude and direction. They identify excursion range (and by extension, mooring line length and anchor spread radius) as an important independent variable. In simulations combining FLORIS wake steering models and NOJ (Jensen) wake deficit models, they model a 3X6 farm and find 22% gain in farm efficiency with their largest excursion range [43]. The authors acknowledge that this efficiency gain is likely inflated due to the unoptimized nature of the control case. An important difference to note between Kheirabadi et al. (2019) [43] and Rodrigues et al. (2015) [25] is that Kheirabadi uses a deeply unoptimized farm, which arranges turbines in such a way that the initial static three crosswind by six downwind turbine array is heavily waked, and the incoming wind is antagonistically mono-directional. Meanwhile, Rodrigues uses a seven crosswind by seven downwind turbine array and uses a data-driven wind rose to model incoming wind, thereby much more accurately simulating real-world conditions and array design constraints. Thus the control case in Kheirabadi has inflated wake losses to begin with, where a real array designer would be more likely to create an array like the one used as the control in Rodrigues' study. This likely accounts for the large difference in farm efficiency gains due to dynamic positioning.

Later, Kheirabadi et al. (2020) do expand their initial array design by simulating a 7-by-7 turbine array, [44]. This simulation is focused on the mechanics of translational excursions, balancing mooring tensions and aerodynamics. A multi-directional wind simulation returned an absolute efficiency gains of 16-22.2%, also finding that the absolute efficiency difference between a dynamic and static farm increased as farm size increased. One interesting result of this study is that the authors measured efficiency gain as a function of wind direction on polar plots, returning a sort of efficiency wind rose [44]. Such plots could be used to help determine the proper neutral position of a dynamic array and likely displacement positions under variable wind conditions. The authors conclude that the technical feasibility of such a farm exists and give mooring design recommendations, but do not address financial feasibility. Kheirabadi et al. (2020) contributes to the creation of FOWFSim-Dyn, which is used as a testing software in later works.

There is a significant body of work considering how to control the repositioning motion of a floating turbine using only aerodynamic thrust on the turbine, by varying yaw and blade pitch angle (and therefore the thrust coefficient). Han et al. (2017) compute the excursion range for a floating turbine controlled only by yaw angle and pitch angle. They found that platforms in still water and a uniform wind field, moored with reasonably stiff moorings, supporting 5MW turbines could at most displace in the crosswind direction about 12 meters under 18m/s wind. They also characterized the Proportional-Integral-Derivative (PID) control settings which produced stable positioning results in a turbine [42]. Then, in 2020, Han et al. continue their work on platform position control, by proposing a Linear-Quadratic-Integral (LQI) control system, and comparing it with three other control schemes, including PID controls. They

found that in time-series wind and wave simulations, LQI controls could use aerodynamic force alone to most accurately and stably displace within a range of a few tens of meters, and did so without additional fatigue loads, relative to other control schemes [45]. Aquino et al. (2020) show that an  $H_\infty$  controller outperforms even the LQI controller under the same metrics, thereby creating a control system which allows individual turbines to position themselves aerodynamically, but with similar motion ranges (constrained by mooring systems) as previous studies [46]. Gao et al. (2022) present a low-level positioning controller which is capable of aerodynamically-driven motion, but can be optimized in either power regulation or power maximization conditions [47], allowing turbines to position aerodynamically even while controlling for secondary parameters. This work was validated using FOWFSim-Dyn (as presented in [44] and [48]) to find power increases of 10-15% at speeds below turbine rating, while maintaining rated power at above-rated windspeeds. It should be noted that here again, an unrealistic farm layout (3-by-1) was used, which forces power losses onto the static farm control case. Jard and Snaiki (2023) and (2024) continue developing control schemes by comparing a PID setpoint control scheme with an Model Predictive Control (MPC) controller in another 3-by-1 farm, and find MPC to more accurately reach the intended turbine position under aerodynamic thrust, while deviating the least from the intended power production of the turbine [49] [50]. Here again, 25% improvement to efficiency is reported, which is likely inflated by the fact that the initial static farm is extremely unoptimal and faces antagonistic wind conditions.

Literature on the topic of the economic viability of dynamic positioning of turbines appears absent, despite the fact that it is typically economic viability that allows for the construction of actual wind farms. The sole exception I've found is by Santarromana et al. (2024)[51], who claim to have carried out a techno-economic analysis of dynamically positioned turbines. There are two problems with how this work relates to this thesis. The first problem is an overlap of vocabulary, where, to one set of researchers, "Dynamic Positioning" refers to a set of turbines that are allowed to move in order to optimize within an array, and to another set of researchers, "Dynamic Positioning" refers to a station keeping system of *thrusters* which have been used by vessels and the offshore oil and gas industry. Such systems have been effective in oil and gas extraction because the energy density of a single production facility can be great (much greater than that of a single turbine or even floating array of turbines), while the water depths can make a bottom-fixed mooring system very expensive [4]. Santarromana et al. have inadvertently collided both sub-fields of naval engineering by proposing a dynamically positioned turbine using dynamic positioning thrusters. They do not claim to have found an increased turbine efficiency while under thrust, and to the contrary, cite literature that thrusting under favorable conditions consumes 20% of the power generated by a turbine, and on average consumes 50%. The study shows that the thruster-driven turbines have minimized Levelized Cost of Energy (LCOE) for medium-rated turbines and deep waters, far from the coast, citing this as a strength of the technology. The authors do not address the need for a hard connection (inter-array and transmission cable) to demand sites, or a method by which turbines might export e-fuels generated in remote oceans (one

suggested use case for this concept). Every model used reveals that such a system would have an LCOE 200-300% that of the directly compared moored turbine. This extra cost is justified in part by the framing of unmoored FOWTs as an environmentally friendly option as it removes mooring lines and anchors from the ocean environment. However, in lauding the environmental benefits of an unmoored FOWT, the authors do not significantly address the financial, technical, safety, or failure risk for unmoored, thruster driven turbines. The authors concede that the noise added by thrusters could be a concern to marine fauna [51]. This research highlights that most systems which consume turbine energy after conversion to electricity in order to generate thrust are unlikely to be economically viable.

## 2.3 Cutting Edge Naval Architecture

Because dynamic FOWF are extremely underdeveloped as a technology, there are a variety of possible design elements outside the standard design schemes for FOWTs that could be utilized, and are thus discussed here.

### 2.3.1 Mooring

There are a number of different mooring-related technologies that could be used to aid in the creation of a cost effective dynamic FOWF. The costs of mooring systems might be reducible by mooring turbines in shared mooring configurations, reducing the number of anchors required. Shared mooring can refer to systems with shared anchors but individual mooring lines only, or systems that have surface lines to connect multiple floaters to a fewer number of bottom-fixed mooring lines, which usually surround a cluster of connected floaters [10]. Such systems thus exert station-keeping force to a number of turbines via fewer mooring lines, and could therefore be more easily influence array layout with fewer driving devices. Shared mooring systems could have a wide variety of topologies, which are selected for stability and cost [10], but could also be selected to generate particular inter-array motion patterns for turbines. Fig. 2.13 shows a selection of topologies investigated by Hall et al. (2022). It becomes clear that, since mooring tensions and weights will add in series, the feasibility of such a system is limited for large arrays - this is visualized by the weight of lines in fig. 2.13, represented by a color gradient.

Single anchor loading (SAL) systems are another potentially relevant mooring technology, which have been used in the oil and gas industry to moor transportation vessels while offloading fuels from extraction platforms [4]. They essentially function as a single mooring line; SALs offer a motion radius of up to 2x the depth of the anchor point, significantly more motion capability than any current or speculative three-line mooring system [12]. Simultaneously, they provide a tension source to generate mooring stability wherever a second persistent force (wind thrust, wave action, or current force) can be found.

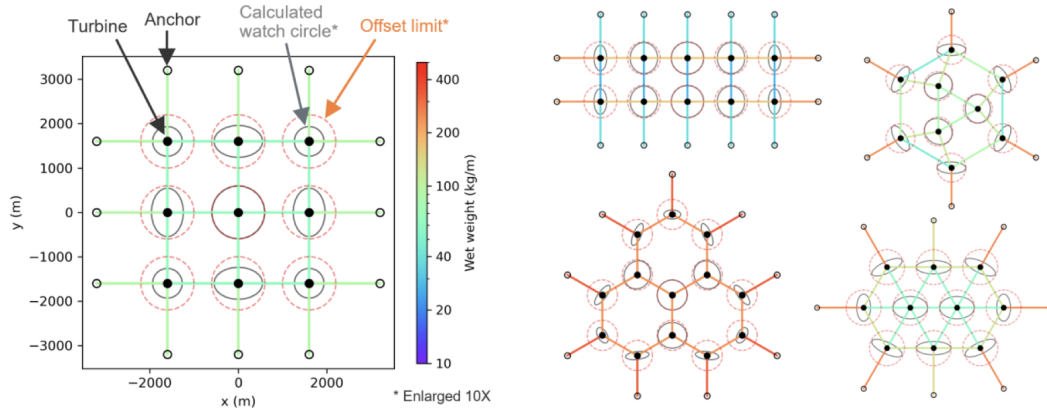


Figure 2.13: From [10], this figure shows a variety of mooring topologies and the line weights required/incurred.

Though not currently in use, there are several concepts for winched mooring systems with some level of control over mooring line lengths, and therefore turbine position [25]. Rather than winches, another speculative mooring idea that could be of future relevance to dynamic farm planners is artificial muscle based active mooring, as presented by Li and Wu (2016), who, recognizing an increase in the degrees-of-freedom floating turbines face relative to their bed-fixed counterparts, investigated the use of artificial muscle linear actuators to better react to structural loads. They found that such a system could be an effective low cost, low power, high bandwidth, and low complexity design [52]. While this investigation was conducted in order to keep platforms stationary and reduce loads, one could imagine this system (or several of these systems linked in series) providing mobility control for offshore turbines.

### 2.3.2 Speculative Motion Options

Given a mooring system which allowed for movement, there are several technologies which could provide locomotive drive to floating turbines, including the already discussed dynamic positioning thrusters [4] [51] and aerodynamic thrust [46] [45]. Another is Flettner rotors, which already see use in ships. Flettner rotors are large tubes which spin, and generate lift according to the Magnus effect, perpendicular to both the wind direction and the tube axis, which allows ships to move at angles closer to the wind than conventional sailing ships. Though there is much interest in the use of Flettner rotors to improve the fuel efficiency of modern engine driven ships or to generate energy on so called "energy ships" [53] no such literature was found on the use of Flettner rotors for wind turbines. Though deeply speculative, it is conceivable that Flettner rotors built around turbine towers or integrated into the floating platform could provide cross-wind mobility for wind turbines, to keep them from entering upwind turbines' wakes.

# Chapter 3

## Methodology

The methodology for conducting this experiment consisted of two main efforts. The first effort was to simulate dynamic farms and compare them to a reasonably optimized static farm, thereby measuring the potential gain in energy production that could be obtained from a dynamic farm. The second effort was to measure the financial feasibility of the dynamic farm, informed by the simulations in the first half of the experiments - this means comparing the monetary value of the gain in energy production to the investment required to create a dynamic farm. The inputs were ERA5 reanalysis data for a variety of sites around the world, farm shapes and sizes, and information from industry experts on naval architecture, costs, materials, and scaling. The goal was to find results which provided evidence for or against the financial viability for a dynamically positioning FOWF. This process is diagrammed in fig. 3.1.

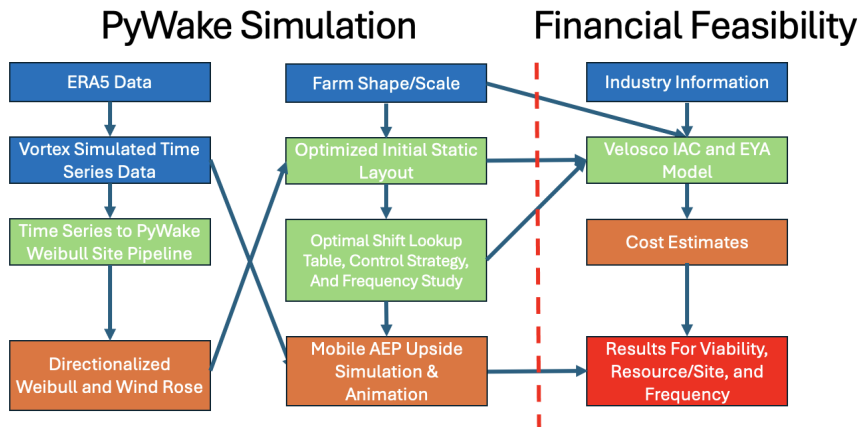


Figure 3.1: This chart shows methodology flow from the inputs (blue), intermediate processing steps (green), interim outputs (orange,) and goal result (red).

### 3.1 PyWake Simulation

In order to gain a full understanding of the potential energy gains for a dynamically repositioning wind farm, realistic array layouts with both static and dynamic turbines were simulated in

Python, specifically the PyWake package, using ERA5 reanalysis time series data for actual sites around the globe.

### 3.1.1 Farm-Level Wake Deficit Model

Much of the modelling for this project used PyWake [11], a Python package for high-level wake-deficit model farm simulation. This software is created by Wind Energy DTU, a team out of Technical University of Denmark. All code is accessible via GitHub, with details in Appendix A.

#### Wake-deficit Model

A wake-deficit model is a simplified or approximate model for how a turbine wake develops, including the extent or radius of the wake, and the wind speed reduction generated by the wake as a function of the distance from the waking turbine. PyWake has the capability to use a number of different wake-deficit models to calculate farm-level wake impacts, as supported by various validation research. The Niels Otto Jensen (NOJ) Deficit Model [14] provided by the PyWake package was chosen as the wake deficit model. Though this model is old and approximate, it is very simple and fast to run on the limited computation resources available (one 2019 MacBook Pro laptop). The model is based on fundamental physics and data from observed wakes [14]. This simplicity was essential to being able to test and run code in an efficient manner, as the wake calculations happen once per iteration, per turbine, and a single run of a dynamic farm can employ millions of iterations over hundreds of turbines. Furthermore this model or slightly modified versions of it are used throughout relevant literature, providing a good basis for comparison. Several other models are offered by PyWake, including a variety of Gaussian deficit models, the G.C. Larsen model, and modified NOJ models. These were not used as they added time complexity to the simulation. In addition, while some of these models are far more accurate in the near wake, they all hold decent accuracy for the far wake, and of them, the NOJ model gives the lowest wind speed deficit along the wake centerline, at any point behind 4D from the waking turbine (see fig. 3.2); this makes the NOJ model the most conservative option for testing a dynamic farm.

The NOJ model assumes a linear wake ( $r \propto x$ ), and solves for momentum conservation. This gives the wake a trapezoidal shape (with the smallest parallel side of the trapezoid being the plane of the turbine rotor). The wake is found to have a velocity according to the following deficit equation,

$$V = U * \left( 1 - 2a * \left( \frac{r_0}{r_0 + \alpha x} \right)^2 \right), \quad (3.1)$$

where  $U$  is the initial free wind velocity,  $r_0$  is the wake radius, initially equal to the radius of the turbine rotor,  $x$  is the downstream distance from the turbine, and  $\alpha$  the entrainment constant equal to 0.1 [11]. PyWake developers note that this model is only valid in the far wake; this study doesn't place turbines in the near wake, so the model should be sufficient

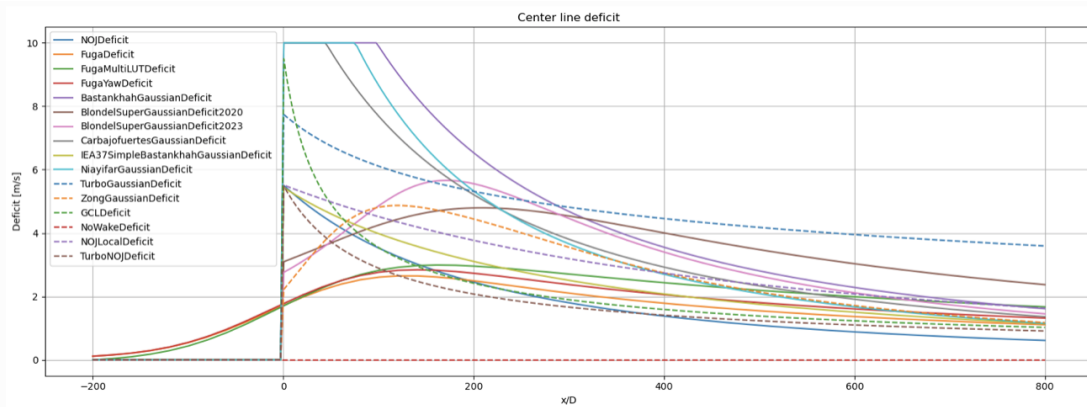


Figure 3.2: From [11], this plot shows the centerline wind speed deficit as a function of distance from the turbine. In the far wake (beyond  $\frac{x}{D} = 400$ , the NOJ model has the lowest deficit, and therefore the highest wind speed, least wake effect, and worst hypothetical efficiency boost for a wake management strategy

for the intended purpose. The wake-deficit model is used by PyWake, in conjunction with wind data (either statistical, directionalized annual wind rose or a time series of wind speed a direction) and turbine location coordinates to determine the wake impact on turbines in a farm.

## Wind Data

ECMWF ReAnalysis v5 (ERA5) data is a dataset of “a large number of atmospheric, land, and oceanic climate variables” which includes global data since January of 1940 through to the present, with data points in a 31k grid, from 137 altitudes, up to a height of 80km [54]. ERA5 data is obtained from the European Centre for Medium-Range Weather Forecasts, produced by its Copernicus Climate Change Service. The wind data used for this study is obtained from a company called Vortex FDC, which offers down-scaled ERA5 wind data; this is to say, Vortex uses ERA5 data to simulate wind conditions at a greater resolution (just 300m) than ERA5’s 31km grid [55]. Vortex has validated its simulated data against in-situ measurements, and found that it generally slightly underestimates actual wind-speeds; however, Vortex meso-scale simulated data typically has a better correlation coefficient and less bias vs. measured wind speeds, than ERA5 macro-scale data [56]. This data is used rather than actual measured historical data as many potential floating offshore sites do not have meteorological masts or turbines which might provide that measured data. Developers of a real wind farm would rely on services like that offered by Vortex to initially scope out a site, then would install physical data collection masts and/or buoys themselves to verify the wind conditions at a site before beginning construction. Since the experiment is simulated and compares two wind farms experiencing the same simulated wind, and considers relative improvement rather than absolute yield, the wind speed bias introduced from Vortex data should not be a source of systemic comparative error. Vortex simulated hourly wind speed data has a mean  $R^2$  value of 0.85 when compared to measured data [56], which industry

standard practices indicate introduces a 2% uncertainty in wind speed [57]. This uncertainty is propagated by creating a time-series file which has wind speeds 2% greater than the original time-series from Vortex, which is then fed through the same algorithm and farm simulation. The difference between the results of the base simulation and the simulation with the increased windspeeds is taken as the uncertainty on annual energy production (AEP).

## Static Models

Static farms were modelled before creating a protocol for dynamic farms, for several reasons. Understanding an optimal static farm was essential for a comparative control case, as comparing a dynamic farm's output to an unoptimized static farm yields little actionable information. This is in contrast to some of the literature, which often use aligned (and therefore heavily wake-impacted and far from optimal) turbines as the control test case. It also informed the control scheme decisions being made for dynamic farms, as the optimizations for a static farm are similar to the instantaneous optimizations being made for a dynamic farm for a particular wind scenario. Finally, static farm modelling helps to highlight which annualized wind scenarios perform worst for a static farm, and therefore helps to inform which wind sites might be best suited for a dynamic farm. Static farms can be modelled with either directionalized Weibull distribution wind data, or wind speed and direction time-series data.

Static farms are modelled primarily with native PyWake. A site object - a data structure which contains data for a directionalized Weibull distribution of windspeeds - and a list of turbine coordinates are given as inputs, and a value for Annual Energy Production (AEP) is taken as an output, with an optional wake map output. A data pipeline was written which allows for site directionalized Weibull characteristics to be measured from the same time-series data given as inputs to time-series tests of the dynamic models. Before running the final static PyWake simulation, a farm must be optimized for the site. This is accomplished by first establishing a rectangular farm which has its intended upwind side facing into the direction of the wind which contains the most energy over a year (the primary wind heading). Then, downwind rows are shifted in small increments and the annual energy production is simulated, generating what is essentially an optimization curve. The shift which produces the greatest energy production (the maxima of the optimization curve) is found; that shift results in a parallelogram-shaped farm, which is treated as an optimized static wind farm, with respect to the statistical wind over a year.

This approach assumes there are no topographical constraints (as the farm is meant to be on the open ocean), nor bathymetry constraints on the farm. It should be noted that this farm shape is optimized by minimizing wake loss (and by extension, maximizing yield) only, and within the constraints of easy-to-calculate geometric arrangements and low farm perimeter to farm area ratio - some recent research indicates more organic shapes may be significantly more cost or profit optimized, on a site-by-site basis [58]. Because they were sites of interest for the dynamic models, due to the structure of their wind roses and high

mean wind speeds, six sites were modelled for a static farm in this way, from sites offshore of Chile, California, Maine, New Zealand, Taiwan, and the current site of the Horns Rev Farm off of the west coast of Denmark. Other than the Horns Rev site, the Taiwan site is the only other site at or around existing offshore projects. The exact coordinates of each site, as well as site characteristics are given in table 3.1, and the wind roses of each site are given in figs. 3.3a-f. These sites were selected by searching for a diversity of wind roses and oscillatory behavior in high-wind (productive), near-shore areas (grid-accessible). This ensured that the later dynamic modelling would capture behavior of a dynamic farm under a wide variety of site conditions, to better characterize dynamic farm performance. Each set of wind conditions was tested with a 25 turbine farm, in 5 rows of 5 turbines each. The turbines tested are NREL 15MW standard turbines, which is primarily represented in the algorithm by the power curve published by NREL[59][60]. This turbine was chosen because it is a standard reference turbine and therefore makes for a good comparative choice against other literature and industry turbine designs, while still representing an average turbine of the 15MW scale. It was important that the 15 MW turbine be chosen, in anticipation of increasingly large turbines being used for offshore wind [59]. For these tests, the turbines were initially spaced 5D (five rotor diameter lengths apart) perpendicular to the incoming wind, and 7D in parallel to the incoming wind, an industry typical spacing scenario, and then subjected to the shift-optimization. The model output was treated as the baseline annual energy production for a farm with the given wind conditions.

Table 3.1: Table of relevant characteristics at each of the six sites modelled.

Site	Latitude	Longitude	Country	Primary WD (deg)	Avg WS (m/s)	Wind Character
Chile	-25.00	-70.00	Chile	30	7.9	Narrow/Bifurcated /Semidiurnal
New Zealand	-37.41	178.68	New Zealand	270/160	9.26	Broad/Bifurcated
HornsRev	55.49	7.84	Denmark	240	10.98	Broad
Maine	42.94	-67.32	United States	210	10.23	Broad/Mono
California	33.87	-120.74	United States	320	8.84	Mono
Taiwan	24.67	120.05	Taiwan	30	10.53	Narrow/Mono

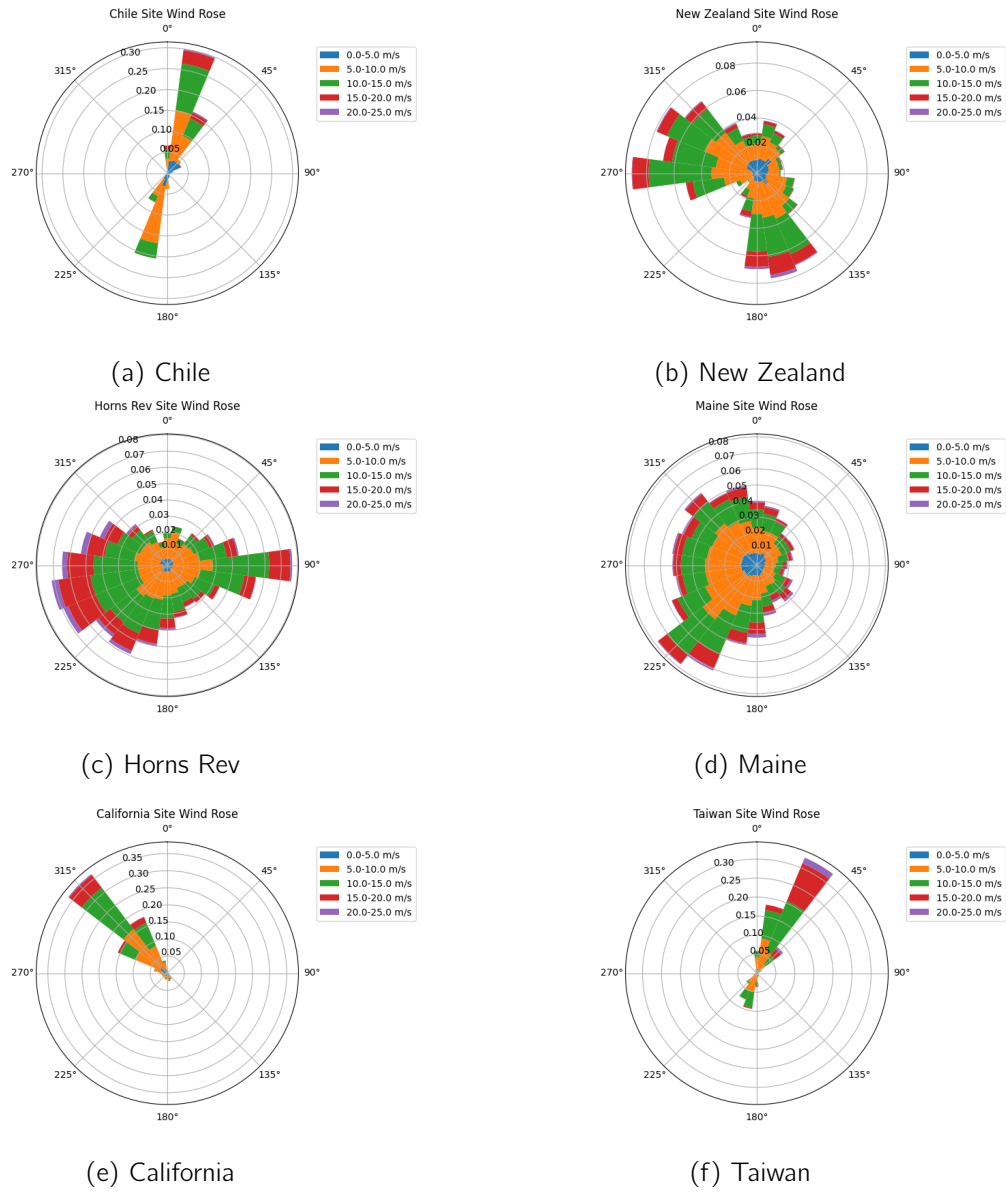


Figure 3.3: Wind roses for each of the six sites considered in the study, generated with the author's data pipeline and PyWake.

## Dynamic Models

Dynamic farms cannot be modelled with directionalized Weibull distribution wind data, as their position shifts relative to incoming wind and so a direct hour-to-hour simulation, rather than a statistical simulation, is required. Dynamic farms are therefore always modelled in reference to time-series data of wind speed and direction. Links to all code for the following algorithm can be found in Appendix A:

1. Initial Conditions: The farm begins in its static-optimized parallelogram shape. For each possible wind direction (granularity of 1 degree of wind direction), the optimal row-wise shift distance of the parallelogram farm is calculated and stored in a lookup

table for computational efficiency.

2. Control Scheme: In order to better understand what frequency of movement was required to have a feasibly useful dynamic farm, each site was tested with direction sensitivities of  $1^\circ$ ,  $5^\circ$ ,  $10^\circ$ ,  $20^\circ$ ,  $40^\circ$ , and  $90^\circ$ . The time series data is split into chunks of similar wind conditions: a new chunk is started when the difference between the current wind direction and the next wind direction in the time series exceeds the sensitivity setting. Thus, the more sensitive ( $1^\circ$  being the *most* sensitive), the higher the frequency of turbine motion within the farm. The wind direction in the first hour of each chunk determines the farm optimization shift used for each chunk. This simulates a farm operator with knowledge only of the current weather conditions and farm state, rather than any future states/conditions. That shift distance is applied in the clockwise crosswind direction, so through  $360^\circ$  of wind, the turbines are simulated as if they can move unconstrained in two dimensions. The simple geometry of the system keeps turbines from colliding, and keeps computational runtime low, probably at the expense of generating suboptimal layouts. Though not done for this experiment, a future researcher could investigate improving this method by simulating weather forecast input to the control scheme, simply by picking the mean wind direction for any time chunk, rather than the first wind direction of the chunk (or any other anticipatory algorithm). Its also important to note that in this simulation, the transition period as turbines move between positions is not considered - this could also be included as future improvements, both as a mechanical simulation of how (and how fast) turbines might move, and as a time-resolution improvement.
3. Time Step: The first chunk of the time series is simulated with the pre-calculated farm shift. The yield is normalized against the length of the chunk. The next chunk is selected and the process is repeated.
4. Annual Yield: The normalized yield of each simulated chunk is added to generate the total yield of the dynamic farm. The dynamic yield is compared to the static yield.
5. Uncertainty Analysis: The algorithm is re-run with time series wind data which has 2% additional wind speed, per the statistical validation provided for Vortex [56], then converted to wind speed uncertainty according industry guidelines from [57]. The initial yield *gain* is compared to the output *gain* from the uncertainty modified re-run algorithm. The percent difference between these two gains is taken as the uncertainty of the results. For example, if the initial data found a 2% gain in yield, and the re-run found a 2.2% gain, the result would be 2% yield gain, with an uncertainty bound of 10% or 0.2% *gain*.

Each site was tested with according to this protocol, with the same initial farm design as the static model, a 25 turbine, 5 by 5 turbine array, using the NREL 15MW standard turbine, with 5D crosswind spacing and 7D downwind spacing.

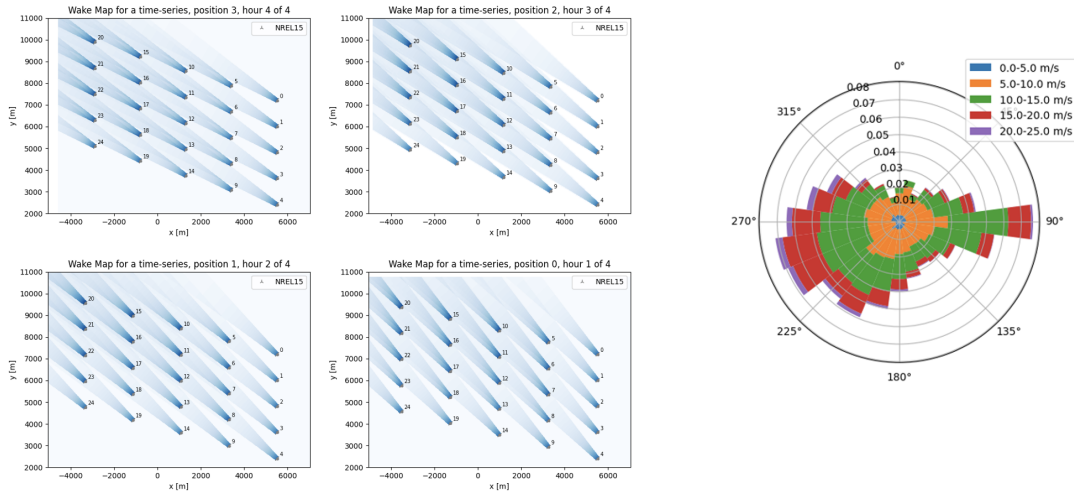


Figure 3.4: The following are three sequential wake maps of a dynamic farm as it changes over time to maintain optimization in shifting wind conditions. From position 1 through position 4 (over four hours), the wind shifts from ESE to SE, and the turbines slightly adjust position to better accommodate wake effects. Wake intensity is shown by the intensity of blue hue. The right-side figure is the wind rose for the site.

## 3.2 Financial Feasibility

Discussion of financial feasibility of dynamic repositioning turbines has been largely absent in the current literature. Having calculated a realistic annual yield boost due to dynamic farms under a variety of conditions, it was important to measure the benefits of the dynamic farm against its costs.

### 3.2.1 EYA Analysis

Once the potential for yield improvement was established and quantified, the extra generation in GWh was converted to dollars by multiplying by the 2024 UK government CfD strike price. Currently, that price, for floating offshore wind (which is specifically subsidized in the UK via the strike price mechanism), is a range from 116£ to 176£ per MWh [61]. The average of these prices, 146£/MWh was used, and then converted to dollars, which at the time of writing, was subject to an exchange rate of GBP:USD of 1.29. Thus, the annual increase in yield of the farm due to dynamic turbines was quantified as an additional cashflow in USD. Using those values (for each site, at each wind direction sensitivity setting), NPV was calculated using a discount rate of 7.5% [62]. Using this cashflow and NPV, an estimate was made of internal rate of return and payback period for each site and motion frequency combination. Sites and frequency combinations that resulted in energy yield loss were considered to have no payback period.

### 3.2.2 CapEx Models

As little work has been done assessing the financial feasibility of a dynamic positioning farm, it was determined that the farm modelled for CapEx purposes should be amongst the simplest and most technologically developed designs, rather than the more speculative designs discussed in chapters 2 and 5. Therefore the CapEx costs found in this study are specific to a single design case, in which each turbine has three taut leg polyester mooring ropes and navigates by winches pulling in or paying out on these ropes. This design was chosen for the CapEx model because it was simple to model, and relied the least on speculative technology. This sort of design concept belongs to one of two proposed moving-turbine mooring topologies proposed by BW Ideol in 2014 [25]. CapEx models created by Velosco Energy (who advised this dissertation) were used to estimate CapEx along with bottom-up calculation based on assumed turbine design characteristics and material costs.

The fundamental assumption in estimating the *upgrade* cost of deploying a dynamic wind farm was that the maximum displacement of a turbine from its original position, and the effect this would have on mooring and inter-array cable (IAC) systems would be the most significant added cost components. In addition, the operating assumption of the CapEx analysis was that cost variance was largely a function of the range of motion of turbines. Since several of the simulated sites achieved their energy yield uplift with a maximum excursion of roughly 700 meters, this was selected as the largest motion range for CapEx calculations. Literature discussing the use of aerodynamic thrust does not consider excursion ranges at this scale, reinforcing the assumption that such a system would be driven by other methods, in this case, winches. Because moorings are most effective when the angle between the mooring line and vertical is largest, 700 meters of motion also stipulated a minimum water depth limit of 2000 meters - exceeding this ratio of depth:excursion range results in too small an angle between the mooring line and vertical, and results in a loss of mooring restoring force [12].

#### Rope Mooring

Based on specifications from industrial naval engineers at Apollo Engineering, it was assumed that the polyester rope required would be in excess of 100mm in diameter and be capable of a pull strength of at least 200 tonnes, and a braking strength of 800 tonnes [12]. The geometry of the rope system was analyzed to determine how much excess rope would be required to accomplish motion of a platform. Of three mooring lines, for any motion, at least one must pay-out. Therefore, the extra rope required for a mobile turbine for a given range of motion, is the total length of the longest pay-out possible, less the original length of the mooring line. A sample of this geometry is available in fig. 3.5.

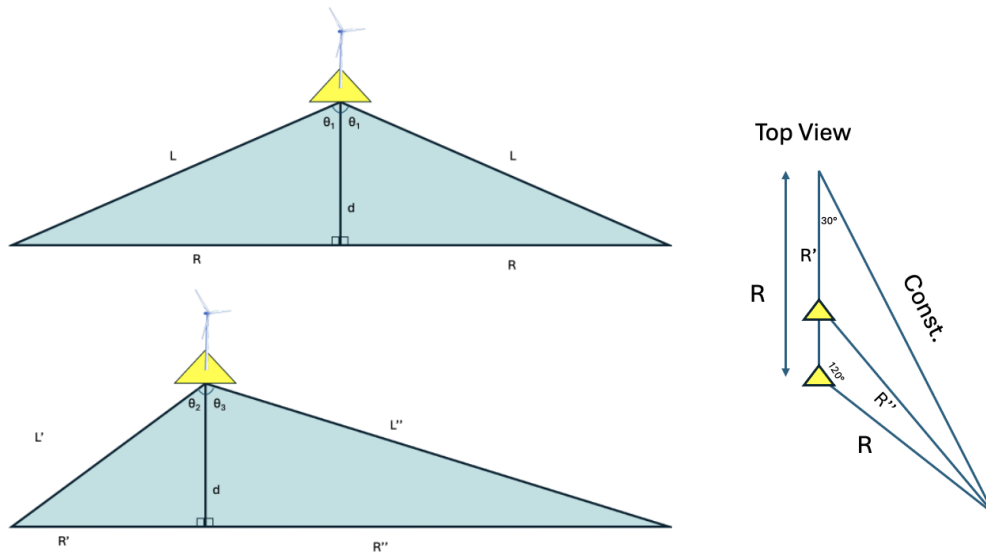


Figure 3.5: Sample 2D geometry governing the line lengths of paying-in and paying-out mooring lines. Here,  $R$  is the initial anchor radius,  $L$  is the initial line length, and  $d$  is the water depth.  $R + \text{motion range} = R''$  and  $L''$  is the longest line length required in the system. In actuality, the 3-Dimensional nature of the problem complicates this geometry, as one of these triangles is set at an angle out of the page, and that angle changes with the motion of the turbine, as is visible from the top view.

By setting maximum values for the excursion range ( $R - R'$ ) as well as upper and lower angle tolerances on  $\theta_1$  and  $\theta_2$ , as was appropriate for various mooring and operational scenarios, a series of mooring line lengths was determined. Mooring line was estimated to have a cost of \$1,000 per meter, roughly standard for specialized, high-strength, large-diameter polyester line, as validated by Velosco. Specific current market costs were unavailable - though suppliers were approached for quotes, none responded.

### Inter-array Cables

Inter-array cable (IAC) costs are simpler than the mooring ropes, as inter-array cables and their costs will vary roughly linearly with turbine motion range in this case would remain near to the surface. The motion range of the turbines was multiplied by a factor of 1.4 to represent the extra cable length required to create a w or spring shape configuration often used for extendable cables. The materials cost of the cables was multiplied by 1.2 to account for the extra durability and shielding that might be required for dynamic cables that are required to regularly deform as turbines move.

### Winches, Winch Energy, and Expected Downtime Costs

On the recommendations of Apollo Engineering [12], winches with 200 tonne pulling capability were selected, which is needed to overcome inherent line tension as well as wind and

wave thrusts on the turbine while moving it. Though requests for quotes from winch manufacturers were not answered, an estimated cost of \$200,000-500,000 was used for CapEx calculations [12]. Each turbine would require one winch for each of the three mooring lines. Such winches require about 1MW of power to operate, and while in operation, the winches pull at a rate of 100 meters per minute. To generate a conservative cost, it was assumed that each motion made by the winches was to pull the turbine to its most extreme excursion point; for example, a turbine with a maximum excursion of 700 meters was assumed to operate its winches for 7 minutes, at an energy cost of  $7/60$  of a MWh. This energy cost was calculated for a variety of daily frequencies of motion (to align with the scenarios from the PyWake modelling), and then had the same CfD strike price applied to it as the energy yield from the PyWake modelling to quantify that loss economically. In addition, it was assumed that for each motion, the turbine rotor would need to be stopped, requiring ten minutes of ramp-up and ramp-down on either end of a motion. Continuing with the previous example then, a 700 meter excursion cost the turbine  $10 + 10 + 7 = 27$  minutes of down-time. The annual fractional downtime (for various daily frequencies of motion) was then multiplied by the base AEP of the turbines to quantify the economic losses due to turbine down-time. This is done rather than subtracting downtime energy directly, as this method captures the actual wind conditions over a years period and therefore gives a more realistic value for downtime loss. These costs were added, along with the IAC and Mooring Line CapEx costs to generate the farm-wide cost of implementing a dynamic positioning system.

# **Chapter 4**

## **Results**

### **4.1 Static Model Performance Analysis**

The static model is intended primarily for comparison against the dynamic model. As such, it's important that the static model be optimized, so as to compare the dynamic farm to a realistically designed and implemented farm, which would, of course, be optimized by any utility or generation company. Across wind sites, the optimal farm design showed roughly 20% improvement in annual energy yield over a naïve rectangular wind farm. This effectively mirrors efficiency improvements found in the literature ([49], [43]) when previous studies have compared an unoptimal farm layout with a dynamic farm under mono-directional winds. Since this efficiency improvement under single-slide optimization and mono-directional wind had roughly the same efficiency as reported by other studies, this value was taken to indicate that the control case static farm was reasonably optimized for its primary wind heading. Manual tests of the static model also confirmed that PyWake was operating as intended.

### **4.2 Dynamic Model Performance Analysis**

Dynamic farm simulations showed an improvement in AEP across all sites for high sensitivity to changes in wind direction. At lower sensitivity to changes in wind direction, some sites experience significant losses in AEP, rather than gains. This is because when the control algorithm is only allowed to move the turbines for particularly drastic shifts in the wind, the turbines get stuck in configurations less optimal than their static counterparts, and can remain there for a long time. Some sites maintain some level of improvement in AEP, even at low frequency of movement. The best case scenarios resulted in 2.4% increased AEP at high wind direction sensitivities, and 2.0% increased AEP at low wind direction sensitivities. These results are summarized in fig. 4.1.

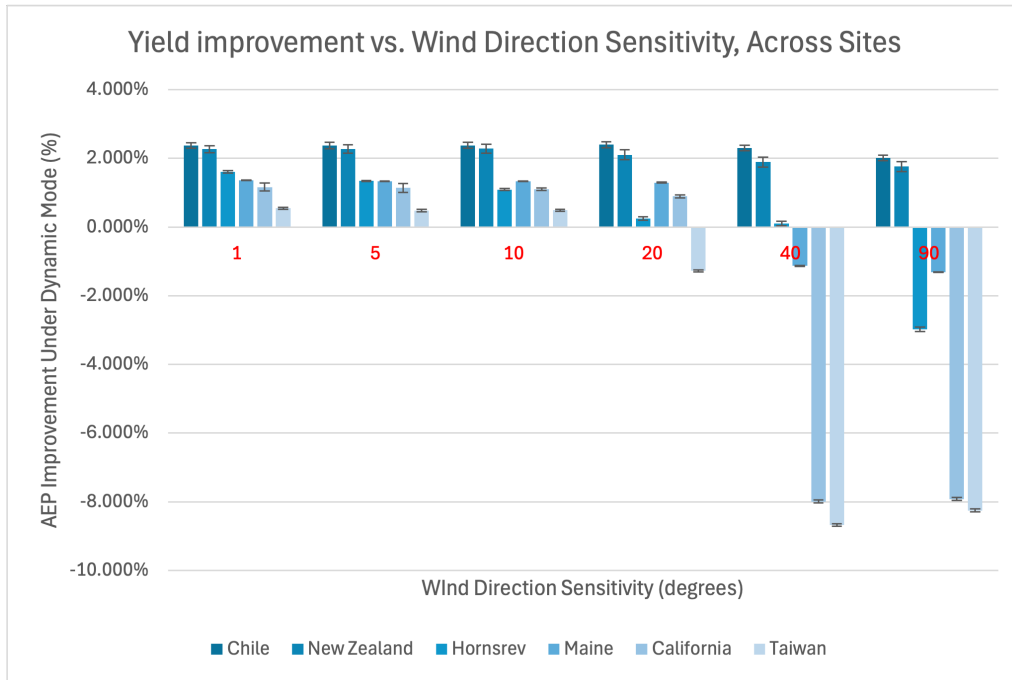


Figure 4.1: This plot shows the annual AEP gained by having a dynamic farm for each site, under different wind direction sensitivity settings. The most sensitive setting,  $1^\circ$  (where the turbines move to a new optimal position if the wind shifts by one degree), yields the highest improvements, while the least sensitive setting,  $90^\circ$ , incurs serious penalties on some sites, but remains better than an optimal static farm for other sites. There are small error bars on each plotted bar representing the uncertainty in yield gain obtained via propagation of the uncertainty in wind data.

The direction sensitivity setting correlates strongly with the number of motions a turbine makes, or the frequency of motion, regardless of the site. This relationship is shown in fig. 4.2. At  $1^\circ$  of sensitivity, the motion is quite frequent,  $\sim 18$  times per day. Because the input time series data was hourly, the maximum possible value was 24 times per day, and it is rare that the wind direction remains within one degree from hour to hour. At a direction sensitivity of  $90^\circ$ , motion is much less frequent, often just once per day.

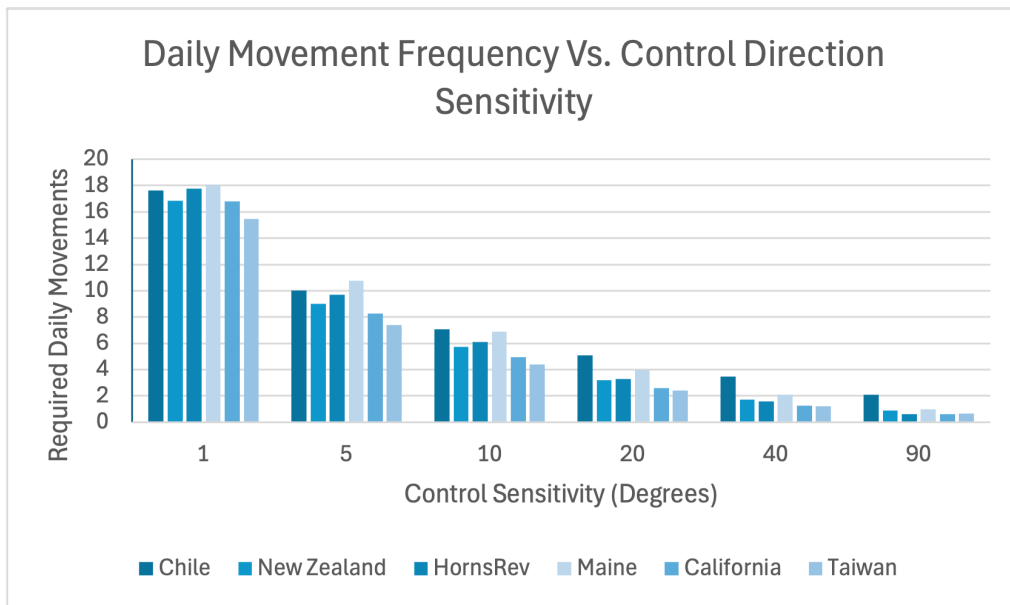


Figure 4.2: This plot shows the average number of movements per day that a turbine at a particular site undertook while operating as a dynamic farm for a variety of wind direction sensitivity settings.

One notable exception to once-per day motion with 40° and 90° sensitivity is the Chile site, which experiences a semidiurnal  $\sim 180^\circ$  flip in wind direction (see fig 3.3), and thus even at 90° sensitivity, would adjust position roughly twice per day.

#### 4.2.1 Site Suitability

Because the AEP uplift from a dynamic farm is so site dependent, it's worth discussing qualitative observations on site suitability. The two sites most consistently generating additional yield across excursion frequency rates were Chile and New Zealand - both of these sites have two distinct "spokes" on their wind roses, and might therefore be called sites with bifurcated wind roses. It makes sense that these sites would enable good performance from a dynamic farm - static farm array designs must optimize for a primary wind direction when considering wake impacts, but bifurcation inherently implies that there are frequent and/or powerful wind conditions at the site for which a static array has not been optimized. While Chile's bifurcated winds were tightly focused into two zones of roughly 30° span each, New Zealand's bifurcated winds were divided into two much wider zones spanning closer to 60° each, and there were regular, if low power, wind conditions outside the two primary zones. The less focused bifurcated wind appears to have slightly diminished the potential gains by a dynamic farm, but not by much. By contrast, the Taiwan site had the worst performance for every wind direction sensitivity. The Taiwan site has the most consistent and mono-directional wind of any site measured, and therefore a static farm is readily optimizeable while a dynamic farm has little purpose. Similarly the California site performed quite poorly as a dynamic farm, and has very mono-directional wind, with just slightly more directional variance than the Taiwan site. The Horns Rev and Maine sites both featured quite broad wind roses which did not have





but not measured in this study, and is also supported by the literature [43]).

Given that all simulated dynamic farms used excursion ranges of at least 700 meters, and the maximum possible NPV of any of the sites studied is well below the CapEx associated with that excursion range, the bottom line result is that the cost of the modelled system exceeds its monetary upside.

# **Chapter 5**

## **Discussion**

As hypothesized, FOWT arrays with dynamic repositioning capability are able to increase yield through adaptation to instantaneous wind conditions. It's also worth noting that on account of simplified models and farm optimization logic, the yield values found are likely conservative. Literature that assesses dynamic farms in relation to optimal static farms typically reports efficiency of about double what was found in this study. However, at face value the results clearly indicate that the system, as modelled, is not financially viable, let alone profitable, supporting the hypothesis that, for now, dynamic farms will not be feasible or adopted by industry. However, this remains one very specific example of how a dynamic farm might function. While the gap between value ( $\sim \$80$  million) and cost ( $\sim \$150$  million) is large, the two quantities are within an order of magnitude of each other, which allows for the possibility of a design case where the value exceeds the cost. Of particularly high cost for the design scheme chosen were mooring costs, winch costs, and motion downtime. Each of these costs is likely to fall in several of the proposed alternative design cases (which of course have their own drawbacks, or are generally more speculative or high risk). The true viability of a future dynamic FOWF remains to be proven or disproven. Particularly as renewable energy is increasingly in demand, if suitable onshore and shallow offshore sites for wind energy are depleted or have development blocked by competing interests, wind developers must be investigating any possible method by which the yield of new or existing FOWFs can be increased. There are many potential ways in which this first iteration could potentially be optimized for better yield or lower CapEx, which should be studied to truly rule out or discover a viable business case for dynamic wind farms.

### **5.1 Future Work**

#### **5.1.1 Input Data**

A major limitation on this study is that the time series wind data from Vortex has hourly time resolution. It is distinctly possible that higher time resolution data would dispute the findings of this study, which has shown that dynamic farms are highly sensitive to the time intervals over which winds shift direction. Finding suitable input data is challenging, because

the sites under consideration do not have any in-situ direct measurement instruments (and no such bifurcated wind, deep offshore sites with anemometers at 100+m altitude exist, to the author's knowledge). Field studies to measure such sites at higher time resolution could be launched, though this seems an expensive venture. Alternatively, new weather models able to simulate higher time resolution versions of Vortex's time series data could be developed, for use in dynamic farm modelling to verify AEP gain findings.

### **5.1.2 Implementing Better Wake Models**

Because of limitations on computational resources, the simplest wake models were used. While these models are roughly valid, more precise AEP results could be obtained with more sophisticated wake modelling. It's possible that more sophisticated wake models would show better AEP gains than found in this study, strengthening the business case for a dynamic farm; it's also possible that more sophisticated wake models would reveal that dynamic farm wake management benefits are less significant than found in this research, and would demonstrate that there is no business case for dynamic farms. PyWake has a number of more sophisticated wake deficit models as well as wind field state solving techniques which would elevate the precision of this work. PyWake can also add farm-wide blockage effects, high resolution turbulence, wake deflection/steering, and superposed multi-source wind effects which would create a more realistic simulation. Implementing these models, even within PyWake, would require greater computational resources, as this study was conducted on an old MacBook.

### **Meandering Wake Models**

Moving away from PyWake, future researchers could also include more complex, but also more realistic wake models that include effects like meandering wake in a time-domain simulation. This is fundamentally different from PyWake in that PyWake models the instantaneous state of a farm or the wake deficit based on statistical wind information, rather than any time-domain simulation. Dynamic farms were modelled in this study by stitching together instantaneous farm states to approximate time-domain modelling, but true time-domain modelling of complex wakes and flow fields could again clarify exactly how beneficial dynamic farms might be, and might be able to inherently model turbines while in transition to intentional excursions, which is ignored in the current model. Some work along these lines, and moving from high-level to low-fidelity CFD modeling has been done by Kheirabadi et al. in the course of development of FOWFSim-Dyn [48][44][43], but still more comprehensive models with stronger attention to realistic array and site scenarios is warranted.

### **5.1.3 Designing Control Schemes**

It must be stated that the control scheme involved in this study is extremely simplified, and likely far from optimal. As the control scheme is a key element of the optimization of the farm, the AEP gains found in this study may be extremely conservative. Qualitatively,

inspection of the wake maps of a dynamic farm often reveals states which appear less than optimal. Furthermore, the motion of the turbines is determined by a simple geometric model that moves rows turbine perpendicular to oncoming wind and assumes this will optimize the farm for a given wind state without causing any turbines to crash into each other. Comparison to other wake management strategies reveals that often, these assumptions do not result in a farm-level optimal state, even when they might optimize at the turbine level [38].

A more sophisticated control algorithm may be able to keep turbines from colliding while also more seriously optimizing farm-level AEP and/or minimizing turbine excursion range (thereby reducing CapEx costs). Control algorithms could also include weather forecasting which could allow the farm to make intelligent decisions on how to configure, even at low motion frequency. Alternatively, forecasting could be used to reduce the need to move turbines, by keeping the algorithm from “chasing” high-frequency weather shifts without ever sitting an optimal position. A significant body of work has built up turbine-level control schemes that allow for aerodynamically-driven turbine motion [46][45][42] - these models should be simulated in conjunction with mooring-mechanical models like that in [44] and array optimization logic as found in [25] and [38].

#### 5.1.4 Modelling Alternative Designs for CapEx and AEP

The value of the AEP gains found in this study and other studies is not insignificant, especially when applied across the entirety of the offshore wind industry and its future growth - finding naval architecture solutions which could support these gains while simultaneously reducing CapEx could help the wind industry to capitalize on these potential gains. The CapEx costs found in this study are specific to a single design case, in which each turbine has three taught polyester mooring ropes and navigates by winches pulling in or paying out on these ropes. This design was chosen for the CapEx model because it was simple to model, and relied the least on speculative technology. It's also worth noting that while there was no attempt to characterize required excursion range in this study - beyond observing the extreme case in an unconstrained optimization farm layout to inform naval architecture design - the CapEx analysis shows that significant cost can be saved by minimizing excursion range. Most studies in the literature refer to excursion ranges 8-15% of that used for the CapEx analysis presented here.

An additional, highly costly, design constraint that was placed on this iteration of testing was the turbine downtime, which assumed that each full excursion required ten minutes of ramp down, seven minutes of non-generating downtime during turbine repositioning, and ten minutes of ramp up. There is no reference to such a constraint in any literature on turbine repositioning, and in fact most of the literature concerns using rotor thrust to control position. Rotor thrusting to reposition is not energetically free, of course, as yaw misalignment and induction over-control both reduce the power a turbine generates. However, this energy loss is accounted for in each of these studies as it directly effects the measured power output of turbines and these studies still demonstrate significant efficiency improvements; Essentially

every study in the literature reports positive effects on efficiency, even those with optimally designed comparative static arrays. Studies considering non-aerodynamic locomotion should determine if it's truly necessary to stall a turbine in order to reposition it under winching or other locomotion. In addition, in conversation with the industry engineers who helped to advise this study, a number of proposals emerged, across a spectrum of reasonable to highly speculative designs. Any of these designs could be modelled for both CapEx and wake avoidance benefits.

First priorities for modelling would be more limited versions of this base design. For instance, the second row of turbines in an array are the most fractionally heavily impacted by wake losses - are there significant AEP gains to dynamically positioning only the second row of turbines, thereby significantly reducing the CapEx, reducing wake deficits on the second row, and steering the second row's wakes away from the third row? What is the effect on the CapEx if turbines in an array are connected by a lattice-shaped shared mooring system, reducing the CapEx effects of increasingly deep waters and possibly collecting winching capabilities into just a few units, rather than three winches per turbine? Could winches be eliminated from the system altogether? There may be ways to generate locomotive forces for turbines that arise passively from the environment, which would eliminate the CapEx cost of winches, along with the significant (but not here quantified) OpEx generated by maintaining high-power winches. Possibly the most feasible, is the aerodynamic thrust method examined by many of the control studies in Chapter 2. This is an attractive option for moving turbines as it uses the thrust they would naturally generate anyway. Using yaw misalignment to steer the thrust may even give controllers joint control over turbine position and wake steering. Another possibly feasible, but likely very site-dependent, design option for passive locomotion is to rudders on the turbine platform that interact with currents or tides to push a turbine, even as the turbine is braced against mooring tension. Similarly, both of these modes of locomotion would likely require some clever design ideas on how turbines would be moored in a way that allowed both motion and control, but didn't allow turbines to drift into each other. Other even more speculative ideas could be considered, like using sails, aerodynamic control surfaces, or Flettner rotors to generate controllable locomotive forces. Flettner rotors, though likely impractical, are intriguing, as they could be wrapped around the already-cylindrical tower structure of a turbine, and naturally produce lift (via the Magnus effect) in a direction perpendicular to incident airflow, the ideal direction for moving turbines out of a wake.

Three mooring lines is an expensive but necessary system to maintain precise station keeping. If dynamic farms didn't need precise station keeping, as the turbines were designed to move anyway, they could significantly reduce CapEx by relying on a single, swivel mounted mooring line, rather than three winching lines. Such systems, called Single Anchor Loading (SAL) systems have been used in the oil and gas industry to moor transportation vessels while offloading fuels from extraction platforms. SALs offer a motion radius of up to 2x the depth of the anchor point, significantly more motion capability than any current or speculative three-line mooring system [12]. This updated mooring design could be combined with any

of the locomotive design elements mentioned above, or even exploit natural current, wave, and wind thrust which are unlikely to be disjoint over the (relatively) small ocean surface area contained within an array. Such a design would likely perform better with or require a weathervaning platform as presented in Serrano et al. (2021) [29]. This would be an unprecedentedly mobile turbine, at a fraction of the costs assessed in this thesis. Fig. 5.1 shows what such a system might look like from above. Clearly this is also very speculative, risky, and would require totally new models to assess both AEP gain and CapEx.

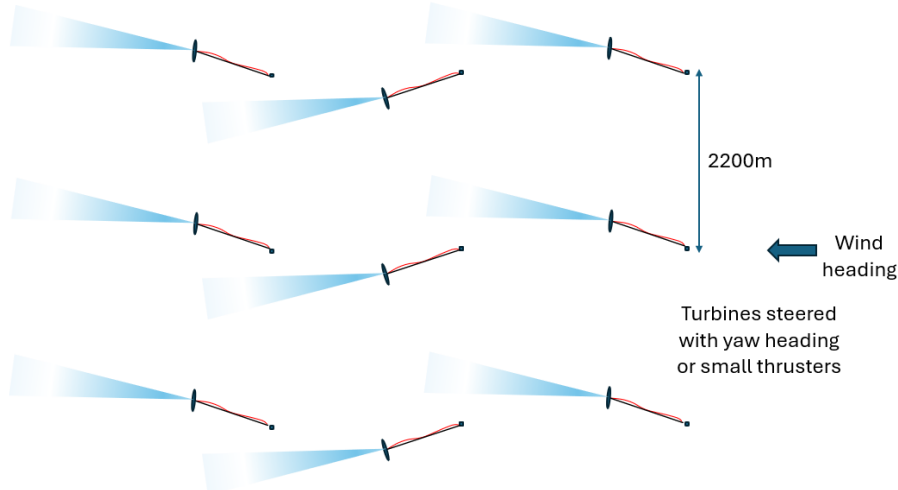


Figure 5.1: This image shows a top view of a design concept by Will Brindley for a dynamically positioned wind turbine array using SAL mooring, in which turbines are using yaw misalignment to both thrust into position and to steer wakes away from other turbines in the array [12].

It is important to recognize that this study has only modelled a single design type for dynamic farms, amongst many potential designs cases. This particular design case is strongly *not* economically feasible. However, this study did find AEP uplift on the scale of other wake management strategies from the simplest, most obvious design case. Dynamic farm design cases ranging from more limited versions of the simple winching design to highly speculative thrust and mooring designs should be modelled for both AEP and CapEx/OpEx to either discover or rule out an economically feasible design configuration.

### 5.1.5 Global Site Survey

The potential for a dynamic farm to improve yields at a site clearly depends on the wind conditions at a particular site. Similarly, the CapEx required to accomplish a productive dynamic farm appears to, in some sites, depend significantly on the frequency of motion, and therefore sites play a significant role in the design and financial feasibility of a dynamic farm. A variety of sites were selected in order to assess what makes a site suitable for a dynamic farm, however, these sites were selected by educated guess and inspection of a wind-speed heatmap and a wind rose preview available on Vortex's website. A global assessment of

high-wind offshore sites around the world would significantly advance the understanding of the potential for dynamic farms to generate additional power. For instance, if sites with bifurcated winds are globally rare, it might indicate that the potential upside of developing dynamic farms is low (and vice versa). A particularly sophisticated site study could estimate a monetary value for the opportunity for increased yield provided by dynamic farms globally, on the basis of number, quality, size, depth, and average wind speed of bifurcated sites globally. A site study could also reveal further wind site categories, and probe their consequences for a dynamic farm - this could potentially include sites with very low frequency wind direction cycles (i.e. seasonal winds) that allow for a dynamic farm that moves every six months, rather than every six hours. Metrics could be developed to quickly assess a site's suitability for dynamic farms, based on wind direction shift frequency and level and narrowness of wind rose bifurcation.

## 5.2 Conclusions

A conservative simulation demonstrates that dynamic positioning of turbines can generate significant AEP uplift, which is supported by the literature. Costs, as calculated according to industry expertise and naval architects far exceeds the value of the AEP uplift here calculated. However, there may be several different designs with better cost outlook; while the design studied here is clearly not economically feasible, economic feasibility is not ruled out. The gaps between the scientific literature on dynamically repositioning arrays and the industry knowledge of costing and feasible design seem quite wide - more work needs to be done to bridge academia and industry on this topic to assess designs for financial feasibility and energetic upside. In addition, little work outside of this study has been conducted to understand how a dynamic farm operates in realistic array layouts and long term wind scenarios, nor indeed which wind roses are best suited to a dynamically repositioning farm. Particularly whilst platform and mooring designs remain non-convergent, a significant opportunity exists to create new technologies to optimize floating offshore wind turbines. In a warming world with ever growing demand for energy, continued investigation into this and any other technique to improve energy yield for offshore wind energy systems is essential.

# References

- [1] A. Lopez, R. Green, T. Williams, E. Lantz, G. Buster, and B. Roberts, "Offshore Wind Energy Technical Potential for the Contiguous United States," Tech. Rep. NREL/PR-6A20-83650, National Renewable Energy Lab (NREL), Aug. 2022.
- [2] C. Allen, A. Viscelli, H. Dagher, A. Goupee, E. Gaertner, N. Abbas, M. Hall, and G. Barter, "Definition of the UMaine VolturnUS-S Reference Platform Developed for the IEA Wind 15-Megawatt Offshore Reference Wind Turbine," Tech. Rep. NREL/TP-5000-76773, 1660012, MainId:9434, University of Maine (UMaine)/National Renewable Energy Lab (NREL), July 2020.
- [3] D. Scicluna, C. De Marco Muscat-Fenech, T. Sant, G. Vernengo, and T. Tezdogan, "Preliminary Analysis on the Hydrostatic Stability of a Self-Aligning Floating Offshore Wind Turbine," *Journal of Marine Science and Engineering*, vol. 10, p. 2017, Dec. 2022. Number: 12 Publisher: Multidisciplinary Digital Publishing Institute.
- [4] K.-T. Ma, Y. Luo, T. Kwan, and Y. Wu, "Chapter 2 - Types of mooring systems," in *Mooring System Engineering for Offshore Structures* (K.-T. Ma, Y. Luo, T. Kwan, and Y. Wu, eds.), pp. 19–39, Gulf Professional Publishing, Jan. 2019.
- [5] D. Gallant, S. Love, and K. Balci, "Velosco In-House NPV Software," Jan. 2021.
- [6] BalmoralOffshore, "Offshore wind cable protection and buoyancy solutions."
- [7] B. G. v. d. Wall, "Wind turbine wake vortex influence on safety of small rotorcraft," *The Aeronautical Journal*, vol. 123, pp. 1374–1395, Sept. 2019.
- [8] B. Sanderse, "Aerodynamics of wind turbine wakes, Literature review," *Energy Research Center of the Netherlands*, Jan. 2009.
- [9] M. F. Howland, S. K. Lele, and J. O. Dabiri, "Wind farm power optimization through wake steering," *Proceedings of the National Academy of Sciences*, vol. 116, pp. 14495–14500, July 2019. Publisher: Proceedings of the National Academy of Sciences.
- [10] M. Hall, E. Lozon, S. Housner, and S. Sirnivas, "Design and analysis of a ten-turbine floating wind farm with shared mooring lines," *Journal of Physics: Conference Series*, vol. 2362, p. 012016, Nov. 2022.

- [11] M. M. Pedersen, P.-E. Réthoré, B. Tobias Olsen, A. Meyer Forsting, P. van der Laan, R. Riva, L. A. Alcayaga Romàn, J. Criado Risco, M. Friis-Møller, J. Quick, J. Peter Schøler Christiansen, and R. Valotta Rodrigues, “PyWake 2.5.0: An open-source wind farm simulation tool,” Feb. 2023. Publisher: DTU Wind, Technical University of Denmark.
- [12] W. Brindley, S. Love, and K. Balci, “Mooring and Cable CapEx and OpEx discussion for dynamic farms with Will Brindley at Apollo Engineering, and subsequent follow-up e-mails.,” Aug. 2024.
- [13] A. Dutton, C. Sullivan, E. Minchew, O. Knight, and S. Whittaker, “Going Global, Expanding Offshore Wind to Emerging Markets,” tech. rep., World Bank Group, International Finance Corporation, Oct. 2019.
- [14] N. Jenson, “A note on wind generator interaction,” *Risø National Laboratory*, vol. Risø-M no. 2411, 1983.
- [15] R. James and W.-Y. Weng, “Floating Wind Joint Industry Project Phase I Summary Report,” tech. rep., The Carbon Trust, Nov. 2018.
- [16] N. Bento and M. Fontes, “Emergence of floating offshore wind energy: Technology and industry,” *Renewable and Sustainable Energy Reviews*, vol. 99, pp. 66–82, Jan. 2019.
- [17] D. R. Houck, “Review of wake management techniques for wind turbines,” *Wind Energy*, vol. 25, no. 2, pp. 195–220, 2022. \_eprint: <https://onlinelibrary.wiley.com/doi/pdf/10.1002/we.2668>.
- [18] R. J. Barthelmie, S. T. Frandsen, M. N. Nielsen, S. C. Pryor, P.-E. Rethore, and H. E. Jørgensen, “Modelling and measurements of power losses and turbulence intensity in wind turbine wakes at Middelgrunden offshore wind farm,” *Wind Energy*, vol. 10, no. 6, pp. 517–528, 2007. \_eprint: <https://onlinelibrary.wiley.com/doi/10.1002/we.238>.
- [19] B. Sanderse, S. van der Pijl, and B. Koren, “Review of computational fluid dynamics for wind turbine wake aerodynamics,” *Wind Energy*, vol. 14, no. 7, pp. 799–819, 2011. \_eprint: <https://onlinelibrary.wiley.com/doi/pdf/10.1002/we.458>.
- [20] J. Baptista, B. Jesus, A. Cerveira, and E. J. S. Pires, “Offshore Wind Farm Layout Optimisation Considering Wake Effect and Power Losses,” *Sustainability*, vol. 15, p. 9893, Jan. 2023. Number: 13 Publisher: Multidisciplinary Digital Publishing Institute.
- [21] K. Thomsen and P. Sørensen, “Fatigue loads for wind turbines operating in wakes,” *Journal of Wind Engineering and Industrial Aerodynamics*, vol. 80, pp. 121–136, Mar. 1999.
- [22] M. Hutchinson and F. Zhao, “Global Wind Report 2023,” tech. rep., Global Wind Energy Council, Mar. 2023.

- [23] C. Cossu, "Wake redirection at higher axial induction," *Wind Energy Science*, vol. 6, pp. 377–388, Mar. 2021. Publisher: Copernicus GmbH.
- [24] S. C. Pryor and R. J. Barthelmie, "Wind shadows impact planning of large offshore wind farms," *Applied Energy*, vol. 359, p. 122755, Apr. 2024.
- [25] S. Rodrigues, R. T. Pinto, M. Soleimanzadeh, P. A. Bosman, and P. Bauer, "Wake losses optimization of offshore wind farms with moveable floating wind turbines - ScienceDirect," Jan. 2015.
- [26] H. Farr, B. Ruttenberg, R. K. Walter, Y.-H. Wang, and C. White, "Potential environmental effects of deepwater floating offshore wind energy facilities," *Ocean & Coastal Management*, vol. 207, p. 105611, June 2021.
- [27] M. Leybourne and S. Whittaker, "World Bank Group Offshore Wind Development Program," June 2021.
- [28] R. Norris, "Global floating offshore wind project pipeline grows by one-third over 12 months - RenewableUK," Oct. 2023.
- [29] J. Serrano González, M. Burgos Payán, J. M. Riquelme Santos, and G. González Rodríguez, "Optimal Micro-Siting of Weathervaning Floating Wind Turbines," *Energies*, vol. 14, p. 886, Jan. 2021. Number: 4 Publisher: Multidisciplinary Digital Publishing Institute.
- [30] A. Alexandre, Y. Percher, T. Choisnet, R. Buils Urbano, and R. Harries, "Coupled Analysis and Numerical Model Verification for the 2MW Floatgen Demonstrator Project With IDEOL Platform," in *ASME 2018 1st International Offshore Wind Technical Conference*, (San Francisco, California, USA), American Society of Mechanical Engineers Digital Collection, Dec. 2018.
- [31] M. Karimirad and C. Michailides, "V-shaped semisubmersible offshore wind turbine: An alternative concept for offshore wind technology," *Renewable Energy*, vol. 83, pp. 126–143, Nov. 2015.
- [32] A. Campanile, V. Piscopo, and A. Scamardella, "Mooring design and selection for floating offshore wind turbines on intermediate and deep water depths," *Ocean Engineering*, vol. 148, pp. 349–360, Jan. 2018.
- [33] K. Xu, K. Larsen, Y. Shao, M. Zhang, Z. Gao, and T. Moan, "Design and comparative analysis of alternative mooring systems for floating wind turbines in shallow water with emphasis on ultimate limit state design," *Ocean Engineering*, vol. 219, p. 108377, Jan. 2021.
- [34] ApolloEngineering and N. Robinson, "PALM Quick Connection System," 2024.

- [35] M. Ikhennicheu, M. Lynch, S. Doole, F. Borisade, F. Wendt, M.-A. Schwarzkopf, D. Matha, R. D. Vicente, H. Tim, L. Ramirez, and S. Potestio, "D3.1 Review of the state of the art of dynamic cable system design," Tech. Rep. 3.1.01, INNOSEA / JDR / RAMBOLL / IREC / COBRA / UL DEWI / WINDEUROPE, Feb. 2020.
- [36] M. Sherry, J. Sheridan, and D. L. Jacono, "Characterisation of a horizontal axis wind turbine's tip and root vortices," *Experiments in Fluids*, vol. 54, p. 1417, Feb. 2013.
- [37] R. Jahantigh, S. M. Esmailifar, and S. A. Sina, "Wind farm control and power curve optimization using induction-based wake model," *Measurement and Control*, vol. 56, pp. 1751–1763, Nov. 2023. Publisher: SAGE Publications Ltd.
- [38] J. R. Marden, S. D. Ruben, and L. Y. Pao, "A Model-Free Approach to Wind Farm Control Using Game Theoretic Methods," *IEEE Transactions on Control Systems Technology*, vol. 21, pp. 1207–1214, July 2013. Conference Name: IEEE Transactions on Control Systems Technology.
- [39] E. Bossanyi, R. Ruisi, G. C. Larsen, and M. M. Pedersen, "Axial induction control design for a field test at Lillgrund wind farm," *Journal of Physics: Conference Series*, vol. 2265, p. 042032, May 2022.
- [40] P. Fleming, J. Annoni, A. Scholbrock, E. Quon, S. Dana, S. Schreck, S. Raach, F. Haizmann, and D. Schlipf, "Full-Scale Field Test of Wake Steering," *Journal of Physics: Conference Series*, vol. 854, p. 012013, May 2017.
- [41] WindESCo, "WindESCo Delivers Wind Industry's First Major Wake Steering Installation," Mar. 2023.
- [42] C. Han, J. R. Homer, and R. Nagamune, "Movable range and position control of an offshore wind turbine with a semi-submersible floating platform," *2017 American Control Conference (ACC)*, pp. 1389–1394, May 2017. Conference Name: 2017 American Control Conference (ACC) ISBN: 9781509059928 Place: Seattle, WA, USA Publisher: IEEE.
- [43] A. C. Kheirabadi and R. Nagamune, "Modeling and Power Optimization of Floating Offshore Wind Farms with Yaw and Induction-based Turbine Repositioning," in *2019 American Control Conference (ACC)*, pp. 5458–5463, July 2019. ISSN: 2378-5861.
- [44] A. C. Kheirabadi and R. Nagamune, "Real-time relocation of floating offshore wind turbine platforms for wind farm efficiency maximization: An assessment of feasibility and steady-state potential - ScienceDirect," July 2020.
- [45] C. Han and R. Nagamune, "Platform position control of floating wind turbines using aerodynamic force," *Renewable Energy*, vol. 151, pp. 896–907, May 2020.
- [46] E. E. Aquino and R. Nagamune, "H<sub>infinity</sub> position transfer and regulation for floating offshore wind turbines | Control Theory and Technology," May 2020.

- [47] Y. Gao, A. Padmanabhan, O. Chen, A. C. Kheirabadi, and R. Nagamune, "A Baseline Repositioning Controller for a Floating Offshore Wind Farm," in *2022 American Control Conference (ACC)*, pp. 4224–4229, June 2022. ISSN: 2378-5861.
- [48] A. C. Kheirabadi and R. Nagamune, "A low-fidelity dynamic wind farm model for simulating time-varying wind conditions and floating platform motion," *Ocean Engineering*, vol. 234, p. 109313, Aug. 2021.
- [49] T. Jard and R. Snaiki, "Real-Time Dynamic Layout Optimization for Floating Offshore Wind Farm Control," Jan. 2024. arXiv:2401.08484 [cs, eess].
- [50] T. Jard and R. Snaiki, "Real-Time Repositioning of Floating Wind Turbines Using Model Predictive Control for Position and Power Regulation," *Wind*, vol. 3, pp. 131–150, Mar. 2023.
- [51] R. Santarromana, A. Abdulla, J. Mendonça, M. G. Morgan, M. Russo, and R. Haakonsen, "Assessing the costs and benefits of dynamically positioned floating wind turbines to enable expanded deployment - ScienceDirect," Apr. 2024.
- [52] Y. Li and Z. Wu, "Stabilization of floating offshore wind turbines by artificial muscle based active mooring line force control," in *2016 American Control Conference (ACC)*, pp. 2277–2282, July 2016. ISSN: 2378-5861.
- [53] B. Elie, B. Bognet, T. Boileau, M. Weber, J.-C. Gilloteaux, and A. Babarit, "Experimental proof-of-concept of an energy ship propelled by a Flettner rotor - IOPscience," May 2022.
- [54] H. Setchell, "ECMWF Reanalysis v5 (ERA5)," Feb. 2020.
- [55] VortexFDC, "Long-Term High-Resolution 10-minute Time Series."
- [56] D. Quantrell and A. Watson, "Offshore Wind Model Validation, ERA5 and Vortex Downscaling," *MetOcean Works Ltd for Vortex*, Aug. 2021.
- [57] S. Love, "Industry Standard Wind Speed Uncertainty from Correlation Coefficient, DNV KEMA guidelines," July 2024.
- [58] D. Cazzaro, A. Trivella, F. Corman, and D. Pisinger, "Multi-scale optimization of the design of offshore wind farms," *Applied Energy*, vol. 314, p. 118830, May 2022.
- [59] E. Gaertner, J. Rinker, L. Sethuraman, F. Zahle, B. Anderson, G. Barter, N. Abbas, F. Meng, P. Bortolotti, W. Skrzypinski, G. Scott, R. Feil, H. Bredmose, K. Dykes, M. Shields, C. Allen, and A. Viselli, "Definition of the IEA Wind 15-Megawatt Offshore Reference Wind Turbine," Tech. Rep. NREL/TP-5000-75698, National Renewable Energy Lab (NREL), Mar. 2020.

- [60] Pduff-code, “NREL 15 MW Turbine Power Curve: turbine-models/Offshore/IEA\_15mw\_240\_rwt.csv at master · github.com/NREL/turbine-models,” Jan. 2021.
- [61] C. Rt.Hon.Coutinho, MP, G. Davies, MP, and S. Rt.Hon.Graham, MP, “Boost for offshore wind as government raises maximum prices in renewable energy auction,” Nov. 2023.
- [62] T. Freyman and T. Tran, “Renewable energy discount rate survey results – 2017,” tech. rep., Grant Thornton, Jan. 2018.
- [63] G. Thornton, “Renewable energy discount rate survey results – 2017,” tech. rep., Grant Thornton Ireland, Jan. 2018.

## Appendix A

# GitHub: Python and Spreadsheets

Github project for all wake simulation code and financial spreadsheets:

<https://github.com/SeamusFlannery/Dissertation.git>

The repository is equipped with a ReadMe.md file explaining the contents of the repository and their role in my work. If the repository is inaccessible, contact [seamusflannery@gmail.com](mailto:seamusflannery@gmail.com) for access. The code most important for understanding the processes of simulating a dynamic farm can be found at /Working\_Scripts/TimeSeriesSim.py. That script takes the basic groundwork and data structures from stationkeeping.py, sites.py, lookup\_table.py, and turbines.py and allows for time series simulations. Animation files were very large and proved troublesome to add to the repository. New animations could take several hours to render on a personal laptop, so there are relatively few examples, but already generated animations are available as mp4 files in directories with the word "animation" in the name. The most important animations are in a directory called "CURATED ANIMATIONS MP4". That directory also contains a PowerPoint file which will display those animations with brief descriptive titles. In general, the other animations most worth watching and comparing are in folders that also have a site name and a number - the number refers to the direction sensitivity that animation is operating under. Viewers may find it interesting to compare the motion of Horns Rev dynamic farm with 1° wind direction sensitivity against the Chile dynamic farm with the same sensitivity. It's also worthwhile watching the algorithmic differences between sensitivity settings for a single site. These sorts of comparisons demonstrate the qualitative findings reported elsewhere in this thesis. Wind data files from Vortex FDC are found in the WindData directory. The excel sheet containing my financial work is also included, by the name "Finance and CapEx, Velosco Validated.xlsx".

## **Appendix B**

### **Zotero Library Link**

IEEE format does not support the sharing of certain information with some source types - for some sources, with limited author, date, or institution data, the IEEE reference may be somewhat insufficient for easily tracking down a source. However, the Zotero library used for this thesis contains information in fields that are not reported in the references list that may be helpful. Therefore, the link to the Zotero library with full citation information is provided here:

[https://www.zotero.org/groups/5594974/ses\\_dissertation\\_seamus\\_flannery/library](https://www.zotero.org/groups/5594974/ses_dissertation_seamus_flannery/library)